論文 / 著書情報
Article / Book Information

題目(和文)	DNA二重鎖切断修復の制御におけるXRCC4タンパク質極C末端(XECT)領域の機能
Title(English)	Function of XRCC4 extremely C-terminal (XECT) domain in the regulation of DNA double-strand break repair
著者(和文)	WANOTAYANRUJIRA
Author(English)	Rujira Wanotayan
出典(和文)	学位:博士（学術）, 学位授与機関:東京工業大学, 報告番号:甲第9900号, 授与年月日:2015年3月26日, 学位の種別:課程博士, 審査員:松本　義久,竹下　健二,塚原　剛彦,林崎　規託,岩崎　博史,冨田　雅典
Citation(English)	Degree:, Conferring organization: Tokyo Institute of Technology, Report number:甲第9900号, Conferred date:2015/3/26, Degree Type:Course doctor, Examiner:,,,,,
学位種別(和文)	博士論文
Category(English)	Doctoral Thesis
種別(和文)	要約
Type(English)	Outline

Function of XRCC4 extremely C-terminal (XECT) domain in the regulation of DNA double-strand break repair

Doctoral Thesis

Submitted by:
Rujira WANOTAYAN

Guided by:
Assoc. Prof. Yoshihisa MATSUMOTO

Department of Nuclear Engineering
Tokyo Institute of Technology
Tokyo, Japan

March 2015

ACKNOWLEDGEMENT

First of all, I would like to show my deepest gratitude to my respected supervisor Dr. Yoshihisa Matsumoto for endless support and guidance academically and experimentally as well as training me to be a complex thinker. I would like to sincerely thank Dr. Akinari Yokoya and laboratory members in JAEA for the guidance and kind support during my internship in June 2013 – September 2013. A special thanks to Dr. Akira Yasui and Dr. Shin-ichiro Kanno of Tohoku University for their kind helps in mass spectrometry analysis. Also, I would like to present many thanks to Mr. Isao Yoda, Cobalt-60 facility operator for kindly helped in irradiation. Moreover, I would like to show my gratitude to professors at Tokyo Institute of Technology for teaching me during my Master and Doctoral study. I would like to acknowledge my laboratory members for giving me good advices and kind supports when I faced problems as well as friendly environment during my stay in Japan. I would like to thank Japan Student Services Organization (JASSO) and Ministry of Education, Culture, Sports, Science and Technology (MEXT) for granting me the scholarship from October 2010 to March 2015. Also, I would like to thank the staffs at Tokyo Institute of Technology for their kind assistance.

I would like to sincerely thank all my previous teachers at Chulalongkorn University and Ekamai International School as well as my supervisors at National Science and Technology Development Agency for the knowledge and experiences which I received in Thailand. Last but not the least, I would like to thanks my lovely family and relatives for the continuous support which gave me the strength to pass

through all the obstacles especially my mother for urging me to keep up with deadlines and my sister for helping me out whenever I needed. I would like to present my sincere gratitude to my aunts for their guidance, unconditional love and care since I was young. Thanks to all my new and old friends for the cheering and supports during my stay in Japan. I really appreciate you all.

ABSTRACT

Function of XRCC4 extremely C-terminal (XECT) domain in the regulation of DNA double-strand break repair

by

Rujira Wanotayan

Tokyo Institute of Technology, 2015

SUPERVISOR: Assoc. Prof. Yoshihisa Matsumoto

DNA double-strand breaks (DSBs) are the most lethal DNA damage to the cells. Two major DNA DSBs repair pathways employed by mammalian cells are homologous recombination (HR) and non-homologous end joining (NHEJ) pathway. Defective repair of DSBs can lead to increased radiosensitivity and elevated risk of carcinogenesis. It is generally thought that the 200 amino acids in the N-terminal region would suffice XRCC4 function. However, the function of C-terminal domain, bearing multiple phosphorylation sites by DNA-PK is still unknown. This study focused on the extremely C-terminal region of XRCC4, which we named "XECT domain". The aim of this study is to elucidate the significance of XECT domain in DNA DSB repair through NHEJ pathway by the systematically generation and analyses of these XECT mutants.

ABBREVIATIONS

APS	Ammonium peroxodisulfate
ATM	Ataxia telangiectasia mutated
BER	Base excision repair
BRCT	BRCA-1 carboxy-terminal domain
CBS	Calf bovine serum
CDKs	Cyclin dependent kinases
Chk2	Checkpoint kinase 2
CMV	Cytomegalovirus
DMSO	Dimethyl sulfoxide
DNA	Deoxyribonucleic acid
DNA-PK	DNA dependent protein kinase
DNA-PKcs	DNA dependent protein kinase catalytic subunit
DSBs	DNA double strand breaks
ECL	Enhanced chemiluminiscence
EGFP	enhanced GFP
FBS	Fetal bovine serum
GFP	Green fluorescent protein
HR	Homologous recombination
IR	Ionizing radiation
kDa	kilo daltons
LB	Luria Bertani broth
LMB	Leptomycin B

MMR	Mismatch repair
MRN	Mre11/Rad50/NBS1
NBS	Nijmegan breakage syndrome
NER	Nucleotide excision repair
NES	Nuclear export signal
NHEJ	Nonhomologous end joining
NLS	Nuclear localization signal
PAGE	Polyacrylamide gel electrophoresis
PBS	Phosphate buffered saline
PCR	Polymerase chain reaction
RAG	Recombination activating genes
RNS	Reactive nitrogen species
ROS	Reactive oxygen species
RPA	Replication protein A
SDS	Sodium dodecyl sulphate
SSBs	Single strand breaks
TEMED	N,N,N'N'-Tetramethylethylenediamine
UV	Ultraviolet
V(D)J	Variable (Diversity) Joining
XLF	XRCC4 life factor
XRCC4	X-ray repair complementing defective repair in chinese hamster cells 4
XECT	XRCC4 extremely carboxyl-terminal

TABLE OF CONTENT

CHAPTER 1
INTRODUCTION

1.1 DNA

DNA, or deoxyribonucleic acid, is the hereditary material in humans and almost all other organisms. The information in DNA is stored as a code made up of four chemical bases: two purines (adenine (A) and guanine (G)) and two pyrimidines (cytosine (C) and thymine (T)). In RNA, thymine (T) is replaced with uracil (U). DNA bases pair up with each other, A with T and C with G, to form units called base pairs. Each base is also attached to a sugar molecule and a phosphate molecule forming a nucleotide. Nucleotides are the basic monomer building block units in the nucleic acids. They are arranged in two long strands that form a spiral called a double helix. There are specific geometry requirements in the formation of hydrogen bonds between the heterocylic amines. The adenine-thymine pair interacts through two hydrogen bonds (A=T) and the guanine-cytosine pair interacts through three hydrogen bonds (G≡C). Most DNA is located in the cell nucleus but small amount are found in the mitochondria. A unique set of 46 chromosomes is stored inside the nucleus in human. Each of these chromosomes consists of long molecule of DNA. The DNA is coiled tightly such that 1.8 meters of it is able to contain in the nucleus. Human DNA consists of about 3 billion bases, and more than 99 percent of those bases are the same in all people. The order, or sequence, of these bases determines the information available for building and maintaining an organism.

An important property of DNA is that it can replicate, or make copies of itself. Each strand of DNA in the double helix can serve as a pattern for duplicating the sequence of bases. This is critical when cells divide because each daughter cell needs to have an exact copy of the DNA present in the parent cell. The DNA molecule unzips lengthwise in order to make a copy of itself. X-ray diffraction data shows that a repeating helical pattern appeared every 34 Angstrom units with 10 subunits per turn. Each subunit occupies 3.4 Angstrom units which is the same amount of space occupied by a single nucleotide unit. In all organisms, the DNA has the same concentration of adenine and thymine and the same concentration of guanine and cytosine. Because A can only pair with T and G can only pair with C, the nucleotides match up with the unpaired bases along the DNA backbone. Like building blocks, they form a new strand that is complementary to the sequence. This forms strands identical to the original strand before it unzipped. The double helix in DNA consists of two right-handed polynucleotide chains that are coiled about the same axis. The DNA double helix stores information in the form of a genetic code. Sections of DNA that contain complete messages are known as genes. (Molecular Biology of the Cell Textbook)

1.2 CELL CYCLE

Cell cycle is the sequence of activities exhibited by cells. The cycle is subdivided into four phases, G1, S, G2, and M. During the cell cycle, checkpoint mechanisms ensure that a cell's DNA is intact before permitting DNA replication and cell division to occur. In G1, chromosomes are not replicated and the cell is not committed to the replication-division process. There is a control checkpoint at the

transition from G1 to S phase. A cell confirms that internal and external conditions are favorable for a new round of DNA synthesis and division, and commits itself to the process. Once the DNA synthesis starts, it only continues to completion. The S stage stands for "synthesis". This is the stage when DNA replication occurs. Sister chromatids are tethered together by specific proteins, cohesins. During the gap between DNA synthesis and mitosis (G2), the cell will continue to grow and produce new proteins. There is another control checkpoint at the end of this gap to determine if the cell can now proceed to enter M phase and divide. During M phase (mitosis), the sister chromatids are separated so that each daughter cell receives a copy of each chromosome. Cell growth and protein production stop at this stage in the cell cycle. Mitosis is much shorter than interphase, lasting only one to two hours.

Mitosis consists of four phases: prophase, prometaphase, metaphase, anaphase, and telophase to produce two identical daughter cells. During prophase, the chromatin in the nucleus begins to condense and becomes visible under the light microscope as chromosomes and the nucleolus disappears. The centrioles begin moving to opposite ends of the cell and fibers extend from the centromeres. Moreover, some fibers cross the cell to form the mitotic spindle. In metaphase, spindle fibers align the chromosomes along the middle of the cell nucleus. This helps to ensure that when the chromosomes are separated in the next phase, each new nucleus will receive one copy of each chromosome. In anaphase, the paired chromosomes separate at the kinetochores and move to opposite sides of the cell. Motion results from a combination of kinetochore movement along the spindle microtubules and through the physical interaction of polar microtubules. In telophase, chromatids arrive at opposite poles of cell, and new membranes form around the daughter nuclei. The chromosomes disperse and are no

longer visible under the light microscope. The spindle fibers disperse, and cytokinesis or the partitioning of the cell may also begin during this stage. In animal cells, cytokinesis results when a fiber ring composed of a protein called actin around the center of the cell contracts pinching the cell into two daughter cells, each with one nucleus. (Tyson and Novak, 2001)

1.3 RADIATION AND DNA DAMAGE

1.3.1 Sources of radiation

Radiation plays an important role in the medical treatment of cancer for more than 100 years tracing back from the use of X-rays to treat cancer in 1896 to the use of radioisotopes and medical linear accelerators as source of radiation in mid-1900 and 1940s respectively. Human beings are exposed to radiation in everyday life. Sources of radiation can be separated into two main categories: natural background radiation source and man-made radiation source. Natural background radiation source includes cosmic radiation, terrestrial radiation and internal radiation. Cosmic radiation is produced by the interaction of charged particles from the sun with earth's atmosphere and magnetic field. Terrestrial radiation comes from the ground and water containing low levels of radioactive materials such as uranium, thorium, radium, radon and their decay products. Source of radiation exposure from radon make up 55% of the sources of radiation exposure reported by NCRP. However, these natural background doses vary from different locations due to the difference in elevation and magnetic field's effect and the difference in concentrations of radioactive materials in the ground for

cosmic radiation and terrestrial radiation respectively. Another form of natural background radiation source, internal radiation is present in all human bodies. These include radioactive potassium-40 in mineral waters, oceans, and earth's crust, carbon-14 in the upper atmosphere, lead-210 in soils, lake, ocean sediments, tobacco smoke and other isotopes. Aside from exposure to natural background radiation sources, human beings are also exposed to man-made radiation sources from medical treatments such as diagnostic X-rays, nuclear medicine and radiation therapy as well as consumer products such as tobacco, building materials, combustible fuels, televisions, smoke detectors, lantern mantles and etc. Major isotopes that are being exposed to would be I-131, Tc-99m, Co-60, Ir-192, Cs-137, and others. Other sources of lesser extent include handling of radioactive materials and residual fallout from nuclear accidents such as Chernobyl or Fukushima Daiichi Nuclear Accident. (Ionizing Radiation Fact Book)

1.3.2 Types of radiation

Two types of radiation are ionizing radiation and non-ionizing radiation. Ionizing radiation is radiation with enough energy to remove tightly bound electrons from the orbit of an atom, causing the atom to become charged or ionized during an interaction with an atom. Non-ionizing radiation is referred to the radiation that has enough energy to move around atoms in a molecule or cause them to vibrate, but not enough to remove electrons.

The ionizing radiation occurs in two forms: particles or waves. There are three main kinds of ionizing radiation: alpha particles, beta particles, gamma rays and X-rays. Alpha and beta particles are directly ionizing as they carry a charge and hence interact with atomic electrons through coulomb forces. Alpha particles include two protons and

two neutrons. They are emitted from the radioactive decay of the heaviest radioactive elements such as uranium-238, radium-226, and polonium-210. Beta particles are fast moving electrons emitted from the nucleus during radioactive decay. Sources of beta particles are tritium, carbon-14, and strontium-90. The high frequency waves like gamma rays and X-rays are indirectly ionizing. This is because it does not carry an electrical charge as the energy of electromagnetic radiation is carried by oscillating electrical and magnetic fields traveling through space at the speed of light.

The health effects of alpha particles depend heavily upon how exposure takes place. External exposure is of far less concern than internal exposure, because alpha particles lack the energy to penetrate the outer horny layer of skin. Internally alpha particle can be very harmful. If alpha emitters are inhaled, ingested (swallowed), or absorbed into the blood stream, sensitive living tissue can be exposed to alpha radiation. Beta particles are more penetrating than alpha particles but are less damaging over equally traveled distances. They travel considerable distances in air but can be reduced or stopped by a layer of clothing or by a few millimeters of a substance, such as aluminum. Some beta particles are capable of penetrating the skin and causing radiation damage, such as skin burns. However, as with alpha-emitters, beta-emitters are most hazardous when they are inhaled or ingested. Exposure to ionizing radiation can be from external and internal sources. Exposure occurs internally from ingesting, inhaling, injecting, or absorbing radioactive materials. No matter it is from external or internal sources, it can irradiate a part of the body or the whole body. Non-ionizing radiation includes electric and magnetic fields, radio frequency (RF), microwaves (MW), infrared (IR), ultraviolet (UV), visible light and extremely low frequency (ELF), for examples, microwave radiation in telecommunications and heating food, infrared

radiation in infrared lamps to keep food warm in restaurants and radio waves for broadcasting. (Ionizing Radiation Fact Book)

1.3.3 Sources of DNA damage

DNA damage is an important cause of genetic disease. The damaging process can be from the exogenous or endogenous sources. Exogenous sources are ionizing and UV radiation, naturally occurring radioisotopes, and numerous genotoxic chemicals present in diet and air, both naturally or as contaminants. Damage caused by exogenous agents may be from physical or chemical mutagens and either in direct or indirect way. An example of the direct physical DNA damage is those induced by UV light. UV radiation produces covalent bonds that crosslink adjacent pyrimidine bases (cytosine and thymine) in the DNA strand. For the indirect physical DNA damage, ionizing radiation (X-rays) initiates DNA mutations by generating free radicals within the cell. These create reactive oxygen species and result in a single-strand and double-strand breaks (SSBs and DSBs) in the double helix. On the other hand, DNA damage can result from endogenous metabolic and biochemical reactions. The two main sources are intracellular oxidative stress and DNA replication errors. Cellular oxidative stress occurred from the metabolic and immunological processes that generate reactive oxygen and nitrogen species (ROS/RNS). ROS/RNS interact chemically with DNA to produce base damages, SSBs, DSBs and complex clustered lesions. Each molecular entity like hydroxyl radicals, hydrogen peroxide and superoxide used different chemical mechanisms to get different types of DNA lesions. The mammalian DNA polymerases have characteristic error rates. The interchangeability between different polymerases

under conditions of stress may introduce alternative polymerases with higher error rates. This makes the cell more susceptible to the introduction of mutations. (Aziz *et al.*, 2012)

1.3.4 Types of DNA damage

Types of DNA damage include base damage, SSB and DSB. SSB may result from damage to the deoxyribose moiety of the DNA deoxyribosylphosphate chain. When a single-strand break occurs, both the nucleotide base and the deoxyribose backbone are lost from the DNA structure. Among these DNA damages, DSB is the most lethal damage to the cells. DSB most often occurs when the cell is passing through S-phase, as the DNA may be more susceptible to breakage while it is unraveling for use as a template for replication. DSBs can be induced by IR both directly and indirectly. The direct damage is through ionization and radical attack while the indirect damage occurred during the process of base damages located close to SSBs or other base damages on the opposite DNA strand. A single particle track can damage more than one sugar or base entity in opposite strands within a distance of less than 10 base pairs from each other. The damaged can be in the form of clustered and non-clustered DNA damage (Aziz *et al.*, 2012).

1.4 DNA REPAIR PATHWAYS

Ionizing radiation induces a large number of lesions in DNA, most of which are repaired successfully by the cell. Ionizing radiation of 1 Gy can generate over 1000 SSBs, 1000 base damages and 20-40 DSBs (Ward, 1990). Although human cells can

adapt to low levels of DNA damage, only one DNA DSB can be sufficient to kill a cell if it inactivates an essential gene or, in metazoan, triggers apoptosis (Rich et al., 2000). Two major DNA repair pathways include homologous recombination (HR) and nonhomologous end joining pathway (NHEJ). Other DNA repair pathways include base excision repair (BER), nucleotide excision repair (NER), and mismatch repair (MMR) which are utilized in the repair of single-strand breaks and base damage.

1.4.1 Homologous recombination (HR)

HR is a DNA repair pathway which precisely repair DNA double-strand breaks using sister chromatid as a template. Sister chromatids are present after DNA replication until cell division. Therefore, HR can work to repair DNA DSBs during late S phase to G2 phase of the mammalian cell cycle only. The fidelity of HR makes it relatively non-mutagenic pathway of repair. HR initiates with extensive 5' to 3' end-processing by the MRN complex and ExoI/BLM complex. ATM and CHK2, a checkpoint kinase phosphorylates MRN complex. Then, BRCA1 regulates MRN complex end-processing. Next, 3' single-stranded DNA (ssDNA) ends are bound by RPA. BRCA2 facilitates the replacement of RPA with Rad51, which forms a nucleoprotein filament leading the 3' ssDNA end of the DNA DSB to search and invade the homologous DNA duplex to create the D loop. The strands are extended by DNA polymerase. The opposite DNA end of the break then anneals to the D-loop to create double Holliday junction. Finally, ends are ligated and the interwound DNA strands (Holliday junctions) are resolved resulting in either crossover or noncrossover gene products (Khanna and Jackson, 2001; Helleday *et al.*, 2007; Summers *et al.*, 2011).

1.4.2 Nonhomologous end joining pathway (NHEJ)

NHEJ repairs DSBs by ligating the two ends and hence, requires ligatable ends. This process maybe associated with limited or extensive additions or deletions of nucleotides at the generated junction, which alters the DNA sequence in the repaired molecule. NHEJ consisted of seven key players: Ku70, Ku86, DNA-PK catalytic subunits (DNA-PKcs), Artemis, X-ray repair complementing defective repair in Chinese hamster cells 4 (XRCC4), DNA ligase IV and XRCC4-like factor (XLF). NHEJ pathways repaired DNA double-stranded breaks in mainly three steps: recognition of the break, DNA end processing and finally ligation of DNA ends. Firstly, Ku70/86 heterodimer recognizes the DSB and binds to the DNA ends, and then it recruits DNA-PKcs to DNA ends forming DNA-PK holoenzyme. This induces inward translocation of Ku. DNA-PKcs protect the DNA ends from exonuclease activities. Upon binding to DNA ends, DNA-PKcs becomes activated by autophosphorylation, which promote end processing by different factors, such as Artemis, polynucleotide kinase/phosphatase (PNKP), DNA polymerases μ and λ, etc. Artemis is an endonuclease involved in the pre-ligation processing of DNA ends. Lastly, Ku recruits XRCC4/DNA ligase IV/XLF complex to DNA ends for ligation process (McElhinny *et al.*, 2000; Lees-Miller and Meek, 2003; Summers *et al.*, 2011). The schematic diagram of NHEJ pathway is shown in Figure 1-1.

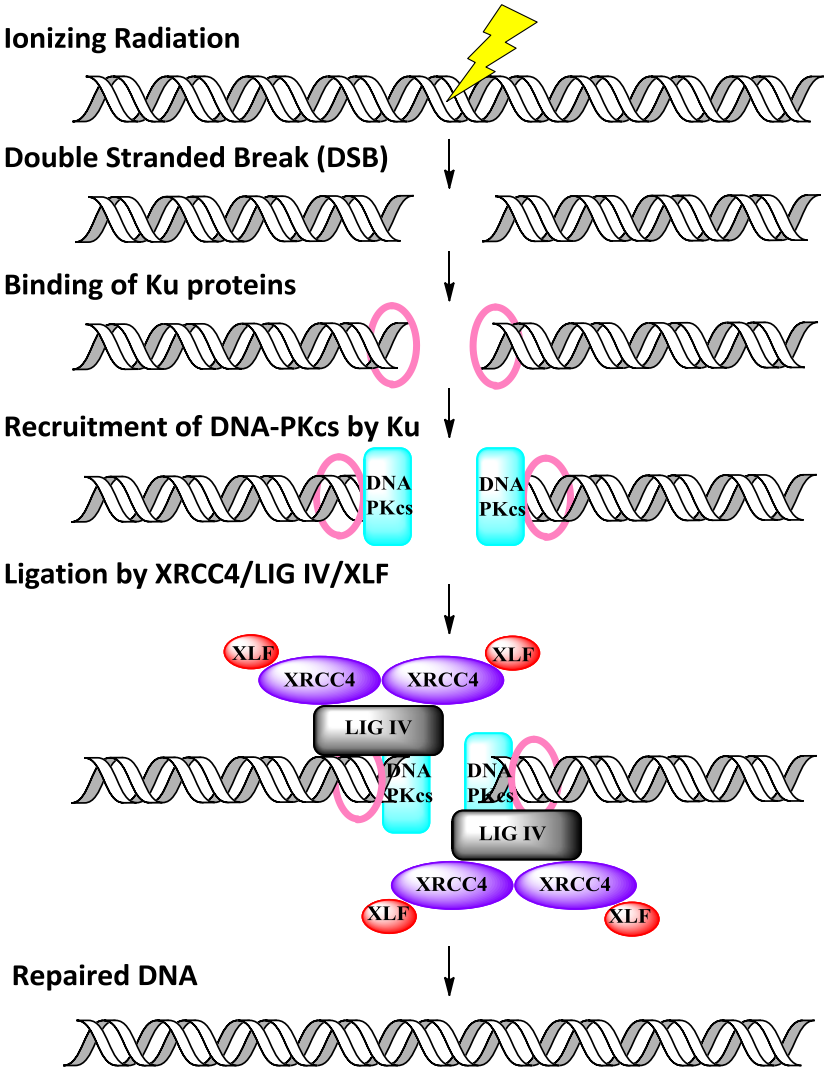

Figure 1 - 1. Schematic diagram of Nonhomologous End Joining Pathway.

1.4.3 Comparison between NHEJ and HR

In mammalian cells, homologous recombination is an error-free pathway which requires a template sister chromatids as the template but works in a slow kinetics, which takes 7 hours or more. Nonhomologous end joining does not require any templates and can join the broken ends directly in a fast kinetic in approximately 30 minutes; however it is an error-prone pathway. HR is nearly absent in G1 and becomes gradually active as cells progress through S phase into G2 phase. On the other hand, NHEJ is active throughout the cell cycle and the activity increases as cells progress from G1 to G2/M. At all cell cycle stages, the overall efficiency of NHEJ is higher than HR. Mao *et al.* (2008) reported that NHEJ of compatible DNA ends where ligation can be done without end processing is six times more efficient than HR where NHEJ of incompatible DNA ends is three times more efficient than HR. They concluded that in proliferating cells, 75% of DSBs are repaired by NHEJ which left only about 25% to be repaired by HR. Compared to HR, repairing by NHEJ is imprecise because the DNA ends are modified before joining, leading to deletions or insertions at the break site, but there is a tradeoff in the efficiency and fast kinetic of NHEJ pathway (Mao *et al.,* 2008). In choosing which DNA repair pathway to repair encountered DSBs in mammalian cells, it depends on the cell cycle stage and the structure of the DNA end as well as other factors such as the signaling pathways (Helleday *et al*., 2007). Interestingly, the appearance of Ku heterodimer at DNA ends is much quicker than HR factors (Kim *et al.,* 2005).

1.5 KEY PLAYERS OF NHEJ PATHWAY

1.5.1 DNA-PK complex

DNA-PK complex is a central regulator of DNA end access during DNA repair through phosphorylation activity. It consists of Ku and its catalytic subunit. Ku is a heterodimer of 70 kDa and 80 kDa subunits (Ku70 and Ku80 respectively) with ring structure (Mimori *et al.*, 1981). Ku binds to DNA ends with high specificity and affinity. It plays an important role in the initiation of NHEJ pathway by recognizing DSBs and recruits DNA-PKcs and other NHEJ molecules to DNA ends. DNA-PK catalytic subunit (DNA-PKcs) is a 460 kDa serine/threonine protein kinase, which is responsible for the kinase activity (McElhinny *et al.*, 2000). DNA-PK is a molecular sensor for DNA damage through phosphorylation of many substrates, such as Artemis, Ku70, Ku80, p53, RPA, XRCC4 and etc. Phosphorylation of these molecules has been reported but it has not been linked to any functional changes *in vivo* (reviewed in Kamdar and Matsumoto, 2011). Phosphorylation of XRCC4 might promote the ligation of DNA ends (Collis *et al.*, 2005).

1.5.2 XRCC4/DNA ligase IV/XLF complex

XRCC4/DNA ligase IV/XLF complex is an essential player in the ligation of DNA broken ends. It consists of XRCC4, DNA ligase IV and XLF. Human XRCC4 is a 336-amino acid protein complementing the deficiency in XR-1 cells. XRCC4 confer normal V(D)J recombination activity and DSB repair activity in XR-1 cells (Li *et al.*, 1995). Biochemical studies lead to finding that it is associated with DNA ligase IV (Critchlow *et al.*, 1997; Grawunder *et al.*, 1997). XRCC4 was reported to be a dimer

based on disulfide cross-linking (Leber *et al.*, 1998). XRCC4 exists as a homodimer *in vivo* (Mizuta *et al.*, 1997). Cells deficient in XRCC4 are associated with radiosensitivity and embryonic lethality (Junop *et al.*, 2000). In the cell, XRCC4 stabilizes DNA ligase IV by protecting it from degradation (Bryans *et al.*, 1999). Moreover, recent finding has found that XRCC4 is required for the recruitment of DNA ligase IV to the repair site in the nuclear (Berg *et al.*, 2011).

Human DNA ligase IV is a 911-amino acid protein whose catalytic domain is highly related to those of other mammalian DNA ligases. DNA ligase IV functions to ligate DNA ends. The binding of DNA ligase IV to XRCC4 is located within its uniquely large C-terminal region that contains a tandem repeat of BRCA1 C-terminal (BRCT) domains, a motif commonly found in proteins involved in DNA repair and DNA damage signaling (Bork *et al.*, 1997). XRCC4-like factor (XLF) or Cernunnos is the newest identified member of NHEJ pathway. It is a 299-amino acid protein, which exists as a homodimer similar to XRCC4 (Andres *et al.*, 2007). From collective studies, Hammel *et al.* (2011) suggested that XLF's interaction with XRCC4 facilitates DNA binding and DNA ligation (Hammel *et al.*, 2011). Very recent study indicated that 10 amino acid region at the C-terminal of XLF is essential for interaction with Ku and for recruitment to DSB (Yano *et al.*, 2011).

Both XRCC4 and XLF are composed of a globular head domain followed by coiled-coil or stalk followed by unstructured C-terminal region. XLF interacts with XRCC4 through their globular head-to-head domains (Andres *et al.*, 2007). Both XRCC4 and XLF exist in solution as a homodimer and can form higher order oligomers like tetramer as shown in Figure 1-2 (Junop *et al.*, 2000). A tetramer results from the packing of the tail-to-tail region of two dimers. XRCC4 and DNA ligase IV bind in

tight complex at the coiled coil domain and the tandem BRCA1 C-terminal (BRCT) motif at the C-terminal, respectively (Critchlow *et al.*, 1997; Sibanda *et al.*, 2001). The stoichiometry of 2:1 of XRCC4 dimer to DNA ligase IV was observed for a stable XRCC4/DNA ligase IV complex in solution (Modesti *et al.*, 2003). The three dimensional structure of XRCC4 interacting with DNA ligase IV BRCT-linker polypeptide is shown in Figure 1-3 (Sibanda *et al.*, 2001).

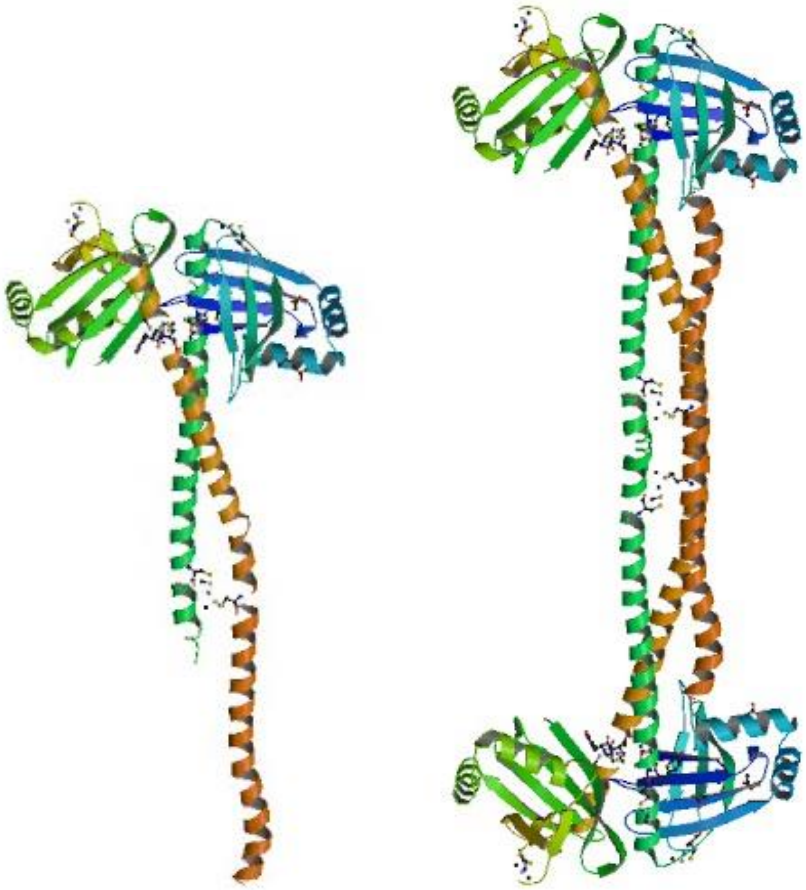

Figure 1 - 2. Crystal structure of human XRCC4 homodimer (left) and tetradimer (right). (Protein Data Bank: 1FU1)

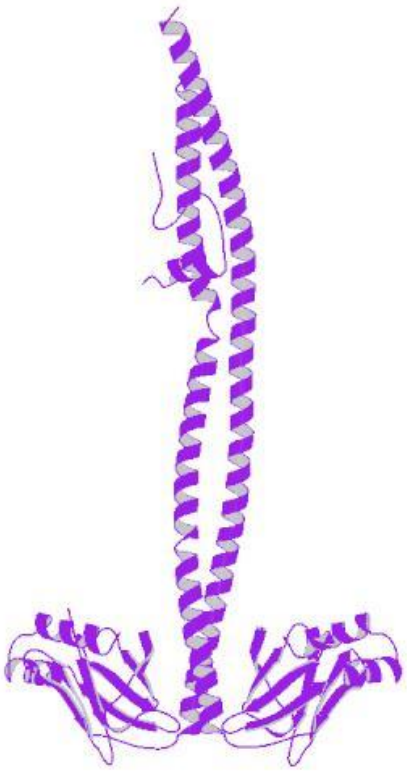

Figure 1 - 3. XRCC4/DNA ligase IV complex. (Protein Data Bank: 1IK9)

1.5.3 XRCC4 extremely C-terminal (XECT) domain

Our laboratory demonstrated that XRCC4 undergo phosphorylation in response to radiation in a manner dependent on DNA-PK (Matsumoto *et al.*, 2000). Since then the identification of the sites of phosphorylation and its role in DSB repair have been pursued. Yu *et al.* (2003) and Lee *et al.* (2004) have analyzed DNA-PK phosphorylation sites in XRCC4 using mass spectrometry and found that all the identified sites lie within the 100 amino acids of the carboxyl-terminal (C-terminal) of XRCC4. They had identified two major phosphorylation sites at serines 260 and 318. However, the function of the C-terminal region of XRCC4 remains unknown. Moreover, many research groups have even ignored the C-terminal region of XRCC4 (Grawunder *et al.*, 1998; Modesti *et al.*, 1999).

XRCC4 protein is highly conserved among mammals but some parts show great diversity. Figure 1-4 shows the conservation score calculated from the conservation of 10 (black) or 20 (red) consecutive amino acids surrounding that position (Wanotayan *et al.*, 2014). As an example, score of 10 shows that all the 10 amino acids around that amino acid are perfectly conserved among five representative mammalian species (*H. sapien, E. caballus, C. familiaris, M. musculus and R. norvegicus*) compared.

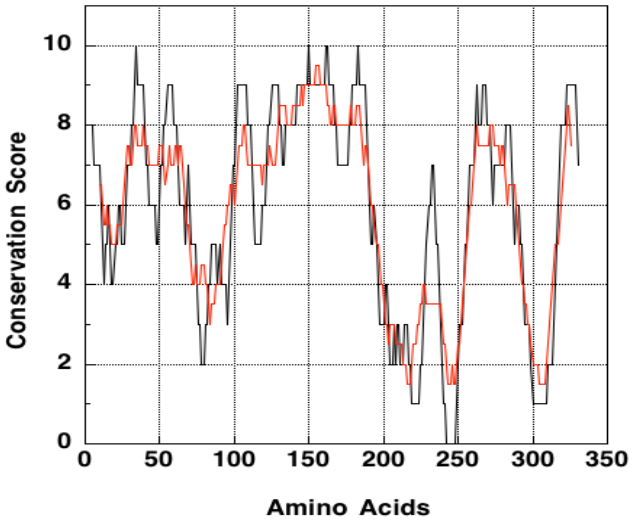

Figure 1 - 4. Conservation of XRCC4 among mammals.

High conservation score regions correspond to several functions of XRCC4, which has been elucidated by many research groups. Based on the research studies so far, full-length XRCC4 with its interacting region can be shown in Figure 1-5.

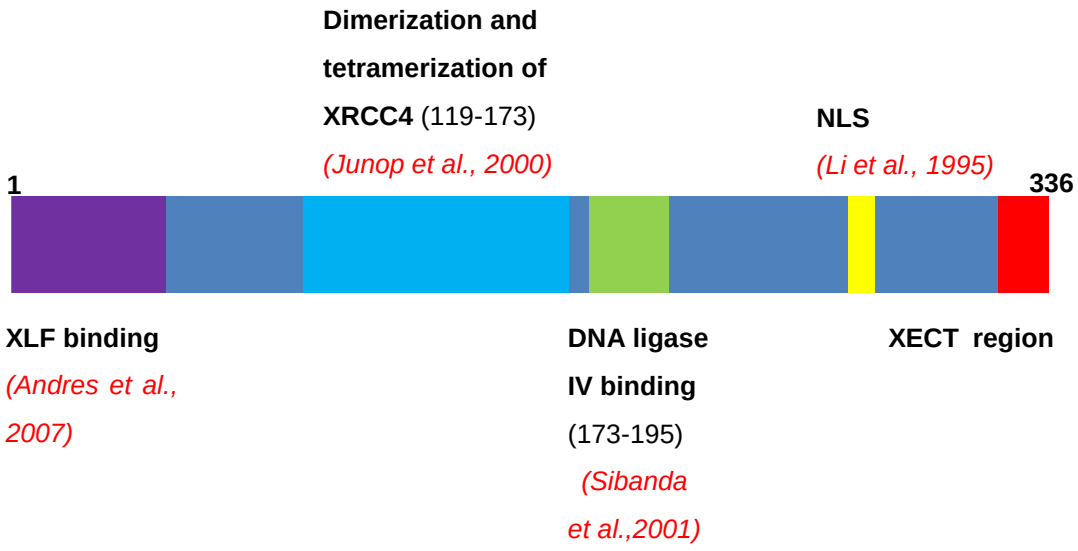

Figure 1 - 5. Diagram of full length XRCC4 with interacting domains.

As much as 16 amino acids among the 18 amino acids in the XECT domain are conserved among five species of mammals compared here. The conservation of amino acid sequence in XECT domain is not limited to potential phosphorylation sites. This XECT conservative region might play a significant role in the XRCC4 function, which is yet to be revealed.

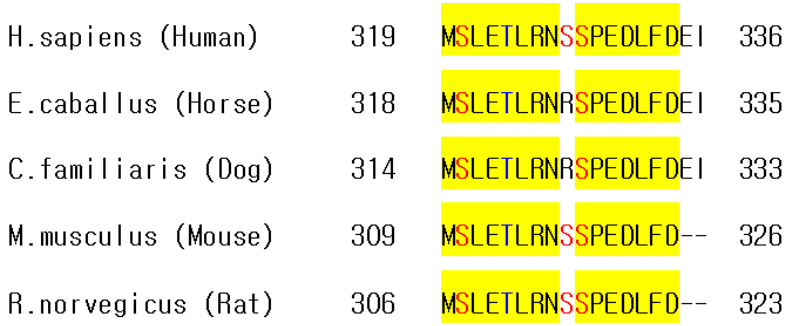

Figure 1 - 6. Sequence alignment of XECT domain (C-terminal 319-336 amino acids of XRCC4).

1.6 THE AIM OF THIS STUDY

Due to the interaction with DNA-PK, a key player in NHEJ pathway, and it is a highly conserved region among mammals, XRCC4 extremely C-terminal (XECT) domain is believed to have some functional significance and play a vital role in the regulation of DNA DSB repair. The aim of this study is to elucidate the significance of XECT domain for DNA DSB repair through NHEJ pathway by generating a series of XECT mutants and to search for the interacting molecules to the XECT domain. These mutants will be analyzed for their proliferation rate, radiosensitivity, posttranslational modification such as phosphorylation and interactions with other molecules. Firstly, functional analysis will be performed for the XECT mutants using biochemical approaches. Then, searching for protein-protein interactions in human cells will be performed.

CHAPTER 2

ANALYSES OF THE CELLULAR CHARACTERISTICS OF CELLS LACKING XECT DOMAIN

(Unpublished part)

CHAPTER 3
EXAMINATION OF THE CHARACTERISTICS OF XECT DOMAIN

3.1 INTRODUCTION

This chapter aims to elucidate the significance of XECT domain for DNA DSB repair through NHEJ pathway by generating a series of mutants, in which each amino acid in XECT domain is changed into others.

3.2 MATERIALS AND METHODS

3.2.1 Cell culture

The derivative of L5178Y mouse leukemia cell line, M10 cell, was obtained from RIKEN cell bank (Tsukuba, Ibaraki, Japan; Code RCB0136) with permission of Dr. Koki Sato (National Institute of Radiologial Sciences and Kinki University). M10 cells are cells deficient in XRCC4 gene, thus radiosensitive (Sato and Hieda, 1979). They were used as the host cell throughout this study. Different types of mutated XRCC4 constructs were introduced into M10 cells for further analysis.

M10 cells were cultured in RPMI1640 medium supplemented with 10% v/v fetal bovine serum (FBS) or calf bovine serum (CBS), 1% v/v of penicillin-streptomycin mixed solution (5,000 U/ml penicillin and 5,000 μg/ml streptomycin) as antibiotics and 10 μM of β-mercaptoethanol. Cells were cultured in 25 cm^2 or 75 cm^2

culture flasks with 5 ml or 20 ml of complete culture media, respectively, in a humidified 5% CO_2 at 37°C.

FBS and CBS were purchased from Hyclone (Logan, UT, USA). RPMI1640 medium and other agents were purchased from Nacalai Tesque (Kyoto, Japan). Addition of small amount of penicillin and streptomycin as antibiotics are used to prevent bacterial contamination of cell cultures due to their effective action against gram-positive and gram-negative bacteria, respectively, which do not affect the mammalian cell culture.

3.2.2 Irradiation

Appropriate number of cells was collected according to the experiment to be performed into 15 ml tube. The cells should be in the log phase. These cells were irradiated in the Cobalt-60 facility with various doses. After irradiation, cells were placed in 37°C incubator for 30 min before placing irradiated cells on ice to slow down the repair mechanism. Cells were harvested for western blotting and kept in deep freezer before use.

Cobalt-60 irradiation source (with reactivity of 222 TBq as of February 2010) with γ-ray energies of 1.17 MeV and 1.33 MeV were used. Cobalt-60 has a half-life of 5.27 years. The dose rate was measured using ionizing chamber-type exposure dosimeter C-110 (Oyo Giken, Tokyo, Japan) and calculated from the best time with consideration of the delay time by the irradiation source.

3.2.3 Analysis of radiosensitivity

Colony formation assay is used to measure the ability of the cells to grow in an independent matter. If the cells are able to proliferate, one cell will form one colony. In this experiment, this assay was used to analyze the effect of various doses of irradiation on M10 cell's survival. Cells were plated in soft agarose after irradiation. The numbers of colonies formed were counted after two weeks. The survival curve was obtained from the following calculations:

$$Plating\ efficiency\ (PE) = \frac{Number\ of\ colonies\ counted}{Number\ of\ cells\ plated}$$

$$Survival\ fraction\ (SF) = \frac{Plating\ efficiency\ of\ irradiated\ sample}{Plating\ efficiency\ of\ nonirradiated\ sample}$$

0.17% w/v of agarose in plating medium containing RPMI1640 supplemented with 15% fetal bovine serum (FBS) or calf bovine serum (CBS) and 1% of antibiotic (Penicillin and Streptomycin) was prepared by first autoclaved 0.17 g of agarose with 4 ml of deionized water at 121°C for 20 minutes prior to mixing with 100 ml of prepared plating medium and pre-warmed in 42 °C water bath to avoid solidification of agarose before plating. $3.0x10^5$ cells were counted using hemacytometer and collected into 15 ml tube before Cobalt-60 irradiation under various irradiation doses. After the irradiation, cells were kept in 37 °C water bath for 30 minutes. Three 60 mm plates were labeled and prepared for each sample. Each irradiated cell sample was diluted into different final concentrations. 0.5 ml of each diluted cell sample was prepared into 50 ml centrifuge tubes and then 12 ml of plating media with agarose solution was mixed

in 50 ml centrifuge tube containing 0.5 ml of each diluted cell sample and dispensed into 3 plates (4 ml/1 plate) with the final number of 30-300 expecting colonies per plate.

3.2.4 Analysis of protein expression

SDS-PAGE or sodium dodecyl sulfate polyacrylamide gel electrophoresis is a technique used to separate proteins according to their polypeptide chain length and charge. The samples were firstly mixed with sodium dodecylsulfate (SDS), an anionic detergent which denatures secondary and non-disulfide linked tertiary structures and gives a negative charge to each protein in proportion to the mass. In addition, β-mercaptoetanol was added to break any disulfide linkage in the protein. SDS sample buffer consisted of 125 mM tris-hydroxymethyl aminomethane (Tris) (pH 6.8), 4% w/v SDS, 20% v/v glycerol, 5% β-mercaptoetanol, 0.05% w/v bromophenol blue and 0.01% w/v crystal violet. The samples were heated to 100 °C to promote protein denaturation helping SDS to bind.

10 % acrylamide gels were prepared by pouring the separating gel solution (1.5 M Tris (pH 8.8), 0.4 % w/v SDS, 10% w/v acrylamide/bis-acrylamide (40:1), 0.1 % v/v tetramethylethylene diamine (TEMED) and 0.03 % w/v ammonium persulfate (APS)) between two glass plates. Once solidified, stacking gel solution (0.5 M Tris (pH 8.8), 0.4 % w/v SDS, 10% w/v acrylamide/bis-acrylamide (40:1), 0.1 % v/v TEMED and 0.075% w/v ammonium persulfate (APS)) was poured over the solidified separating gel. The comb was placed to create the wells. After the gel was solidified, the comb was removed. Occasionally, pre-casted gels with 5-20% gradient of acrylamide concentration were used.

Hand-casted gels or pre-casted gels were prepared prior to the experiment as described above, and then assembled into the gel cassette and placed into the SDS-PAGE tank, which was filled with SDS running buffer. The running buffer should cover the wire in the gel cassette. After that, the samples were loaded into the wells. For the blank wells, sample buffer was loaded. SDS running buffer was added to fill the wells and the middle space to connect the electrodes. SDS-PAGE tank was connected to the electricity and run at 20 mA for 75-90 minutes for one gel and 40 mA for 75-90 minutes for two gels.

Western blotting or protein immunoblotting is an analytical technique to detect the protein of interest in the sample by first separating them by their molecular weight through SDS-PAGE and then transferred them to membrane to be probed by specific antibody to the target protein.

After the electrophoresis was completed, the proteins were electrophoretically transferred from polyacrylamide gel onto 0.45 μm Immobilon P polyvinylidene difluoride (PVDF) membrane (Merck-Millipore, Billerica, MA, USA). The membrane was soaked into methanol for one minute and then submerged into transfer buffer (100 mM Tris, 192mM glycine, 5% methanol) until use. Three filter papers (size 6.5 cm x 9 cm) were soaked in transfer buffer without SDS before stacking on the transfer machine. PVDF membrane was placed on top of the three filter papers followed by the electrophoresis gel. After that, another three filter papers soaked with transfer buffer without SDS were stacked on top. Bubbles between each layer were removed thoroughly. Transfer machine was run at 110 mA, for each gel, for 60 minutes for one gel.

Blocking solution consisting of 1% w/v of skim milk diluted in TBST solution

(20 mM Tris (pH 7.6), 150 mM NaCl and 0.05% v/v Tween 20) was stirred for at least 30 minutes prior to use. After the transfer step was completed, the membrane was transferred to a box containing blocking solution and blocked for one hour or overnight. This step was done to prevent the membrane and antibody interaction. Proteins in the skim milk attached to the membrane where there was no target protein. This helps to reduce the noise in the result.

After blocking, diluted antibody (0.1% v/v of antibody in blocking buffer) was applied to the nitrocellulose membrane. They were incubated with gentle shaking for 1-2 hours or overnight at 4°C. In this experiment, antibody to protein tag such as α-FLAG which can bind to the FLAG tag in the pCMV10 vector or antibody to the target protein itself was used to detect XRCC4 protein inserted in the pCMV10 vector.

As for the loading control, proliferating cell nuclear antigen, commonly known as PCNA, which is present in the cell's nucleus was used to equalize the cell concentration in each loading sample. PCNA Ab-1 (PC10) (NeoMarkers, Fremont, CA, USA) with a concentration of 20 μg/ml was used as the primary antibody and polyclonal goat anti-mouse immunoglobulins (Dakocytomation, Gastrup, Denmark) with a concentration of 1.1 μg/ml was used as the secondary antibody. The membrane was washed after each antibody binding step five times with TBST solution and one time with TBS solution (20 mM Tris (pH 7.6), 150 mM NaCl) for 2, 2, 5, 5, 2 and 2 minutes respectively.

After the membrane was probed with antibody, it was treated with ECL Plus Western Blotting Detection Reagents (GE Healthcare, Buckinghamshire, UK). The solution was incubated for 10 minutes before developing the result with ImageQuant.

3.2.5 Mutagenesis and establishment of stable clones

Mutagenesis is a process in which genetic information is changed resulting in a mutation. There are several types of mutagenesis. In this study, site-directed mutagenesis was performed to change one amino acid of interest at a time to study the functional importance of each amino acid in XRCC4 post-translational modification or analyze their radiosensitivity to ionizing radiation.

3.2.5.1 Vector

In this study, two types of vector were used: pCMV10 vector and pEGFP_C1 vector. pCMV10 vector was used as the vector where normal human XRCC4 cDNA (XRCC4) and deleted C-terminal XRCC4 (K311X) were inserted. pCMV10 vector map was shown in Figure 3-1. The main advantages of pCMV10 are that it contains the strong CMV promoter for high-level constitutive expression in mammalian cells, three times FLAG tag which greatly enhances the detection of low expression proteins upon α-FLAG antibody binding in Western blotting, immunoprecipitation, and immunocytochemistry, and a multiple cloning site (MCS), which is shown in Figure 3-2. Moreover, pCMV10 vector contains neomycin resistant gene which can be used in the stable expression with neomycin selection (G418 sulfate) and β-lactamase gene for ampicillin resistance selection in bacteria.

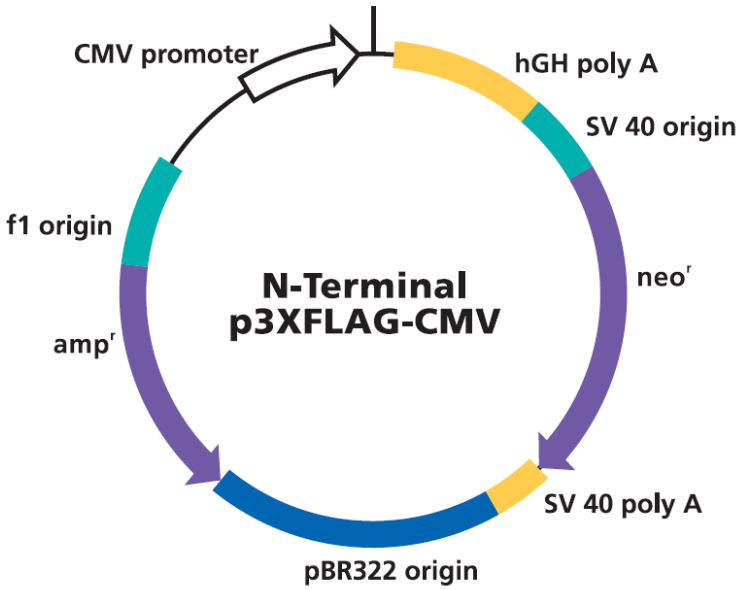

Figure 3 - 1. pCMV10 vector map from Sigma-Aldrich.

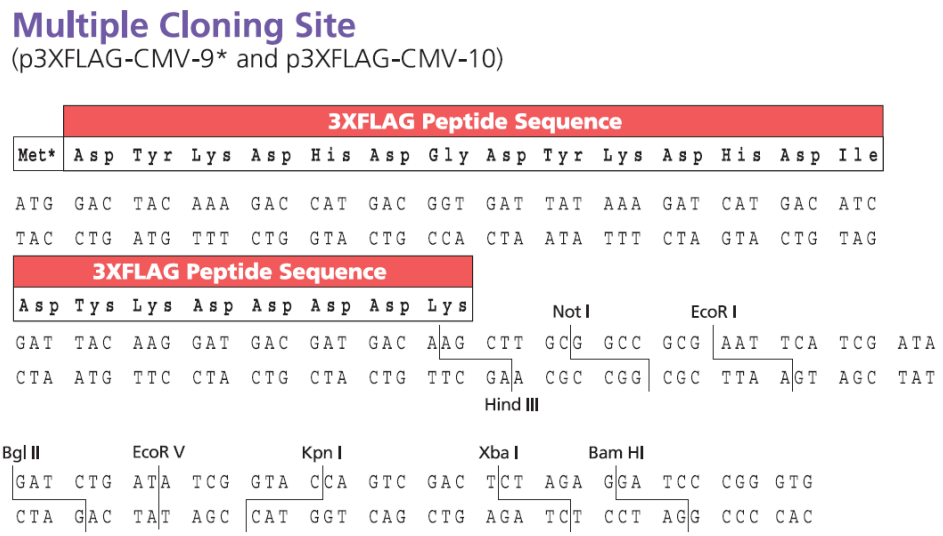

Figure 3 - 2. Multiple cloning site for pCMV9 and 10 from Sigma-Aldrich.

Another vector used in this study was pEGFP-C1, which was used as the vector for different constructs of mutated XECT domain. The vector map for pEGFP-C1 was

shown in Figure 3-3. pEGFP-C1 encodes a red-shifted variant of wild-type GFP that has been optimized for brighter fluorescence and higher expression in mammalian cells. pEGFP-C1 vector also contains a neomycin resistance gene (neo^r) and neomycin/kanamycin resistance gene of Tn5, which permit the selection of a stably transfected eukaryotic cells using G418.

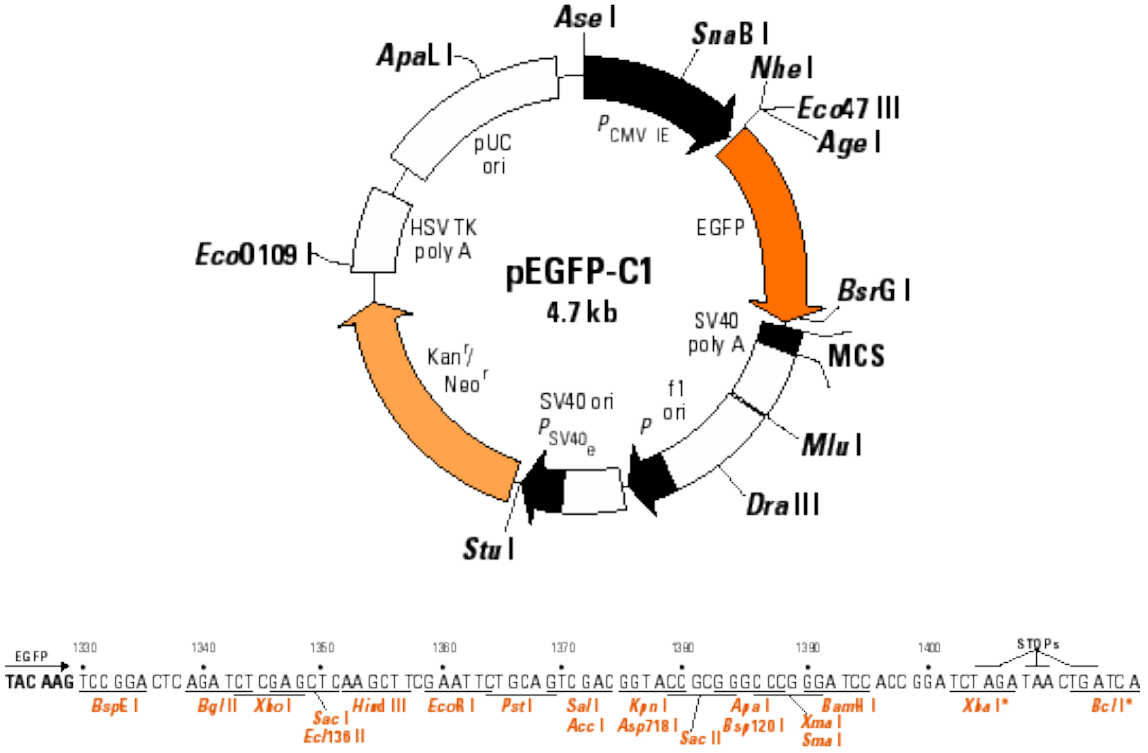

Figure 3 - 3. pEGFP-C1 vector map and its multiple cloning site from Clontech.

3.2.5.2 Primer design

XRCC4 gene's coding sequence contains 1008 nucleotides which codes for 336 amino acids, where 319-336 amino acids are considered as the XECT domain. The

original nucleotide sequence of human XRCC4 in the extremely C-terminal region and the sequence after inserted into pEGFP-C1 vector were shown in Figure 3-4. Mutation positions and amino acids for XECT domain were shown in Table 3-1.

XECT nucleotides [319-336 amino acids]
5' - 1085 ATG TCT TTA GAA ACT CTG AGA AAC AGC AGC
CCA GAA GAC CTC TTT GAT GAG ATT 1136 - 3'

Original human XRCC4 sequence around XECT domain
5' - 1067 CAC ATC TCA GCT GAA AAC ATG TCT TTA GAA
ACT CTG AGA AAC AGC AGC CCA GAA GAC CTC TTT GAT
GAG ATT TAA CAG TCT CAA AAA ATA CTT 1157 - 3'

Human XRCC4 inserted in pEGFP-C1 vector
5' - ...CAC ATC TCA GCT GAA AAC ATG TCT TTA GAA ACT
CTG AGA AAC AGC AGC CCA GAA GAC CTC TTT GAT GAG
ATT CTC GAC GGT ACC GCG GGC CCG... -3'

Figure 3 - 4. XRCC4 extremely C-terminal (XECT) nucleotide sequence.

Table 3 - 1. Mutation positions and amino acids for XECT domain.

Amino acid position	Original Amino acid	Original Codon	Mutated amino acid	Mutated codon
319	Methionine (Met, M)	ATG	Cysteine (Cys, C)	TGT
320	Serine (Ser, S)	TCT	Aspartic acid (Asp, D)	GAC

321	Leucine (Leu, L)	TTA	Tryptophan (Trp, W)	TGG
322	Glutamic acid (Glu, E)	GAA	Leucine (Leu, L)	TTA
323	Threonine (Thr, T)	ACT	Aspartic acid (Asp, D)	GAC
324	Leucine (Leu, L)	CTG	Tryptophan (Trp, W)	TGG
325	Arginine (Arg, R)	AGA	Phenylalanine (Phe, F)	TTC
326	Asparagine (Asn, N)	AAC	Leucine (Leu, L)	TTA
327	Serine (Ser, S)	AGC	Aspartic acid (Asp, D)	GAC
328	Serine (Ser, S)	AGC	Aspartic acid (Asp, D)	GAC
329	Proline (Pro, P)	CCA	Tryptophan (Trp, W)	TGG
330	Glutamic acid (Glu, E)	GAA	Leucine (Leu, L)	TTA
331	Aspartic acid (Asp, D)	GAC	Leucine (Leu, L)	TTA
332	Leucine (Leu, L)	CTC	Tryptophan (Trp, W)	TGG

333	Phenylalanine (Phe, F)	TTT	Tyrosine (Tyr, Y)	TAT
334	Aspartic acid (Asp, D)	GAT	Leucine (Leu, L)	TTA
335	Glutamic acid (Glu, E)	GAG	Leucine (Leu, L)	TTA
336	Isoleucine (Ile, I)	ATT	Tryptophan (Trp, W)	TGG

(E335, I336 mutants were omitted because corresponding amino acids are missing in other mammals.)

In designing the primer, firstly six nucleotides were extended to both 5' and 3' ends of the DNA sequence, and then twelve more nucleotides were extended to 3' ends. Three nucleotides in the middle column of Table 3-2 and Table 3-3 correspond to amino acid number specified on the left.

Table 3 - 2. Original sequences of XECT domain.

	18 nucleotides extended to 5'		18 nucleotides extended to 3'
319	CAC ATC TCA GCT GAA AAC	ATG	TCT TTA GAA ACT CTG AGA
320	ATC TCA GCT GAA AAC ATG	TCT	TTA GAA ACT CTG AGA AAC
321	TCA GCT GAA AAC ATG TCT	TTA	GAA ACT CTG AGA AAC AGC
322	GCT GAA AAC ATG TCT TTA	GAA	ACT CTG AGA AAC AGC AGC
323	GAA AAC ATG TCT TTA GAA	ACT	CTG AGA AAC AGC AGC CCA

324	AAC	ATG	TCT	TTA	GAA	ACT	CTG	AGA	AAC	AGC	AGC	CCA	GAA
325	ATG	TCT	TTA	GAA	ACT	CTG	AGA	AAC	AGC	AGC	CCA	GAA	GAC
326	TCT	TTA	GAA	ACT	CTG	AGA	AAC	AGC	AGC	CCA	GAA	GAC	CTC
327	TTA	GAA	ACT	CTG	AGA	AAC	AGC	AGC	CCA	GAA	GAC	CTC	TTT
328	GAA	ACT	CTG	AGA	AAC	AGC	AGC	CCA	GAA	GAC	CTC	TTT	GAT
329	ACT	CTG	AGA	AAC	AGC	AGC	CCA	GAA	GAC	CTC	TTT	GAT	GAG
330	CTG	AGA	AAC	AGC	AGC	CCA	GAA	GAC	CTC	TTT	GAT	GAG	ATT
331	AGA	AAC	AGC	AGC	CCA	GAA	GAC	CTC	TTT	GAT	GAG	ATT	CTC
332	AAC	AGC	AGC	CCA	GAA	GAC	CTC	TTT	GAT	GAG	ATT	CTC	GAC
333	AGC	AGC	CCA	GAA	GAC	CTC	TTT	GAT	GAG	ATT	CTC	GAC	GGT
334	AGC	CCA	GAA	GAC	CTC	TTT	GAT	GAG	ATT	CTC	GAC	GGT	ACC
335	CCA	GAA	GAC	CTC	TTT	GAT	GAG	ATT	CTC	GAC	GGT	ACC	GCG
336	GAA	GAC	CTC	TTT	GAT	GAG	ATT	CTC	GAC	GGT	ACC	GCG	GGC

Table 3 - 3. Modified sequences of XECT domain.

	18 nucleotides extended to 5’							18 nucleotides extended to 3’					
319	CAC	ATC	TCA	GCT	GAA	AAC	TGT	TCT	TTA	GAA	ACT	CTG	AGA
320	ATC	TCA	GCT	GAA	AAC	ATG	GAC	TTA	GAA	ACT	CTG	AGA	AAC
321	TCA	GCT	GAA	AAC	ATG	TCT	TGG	GAA	ACT	CTG	AGA	AAC	AGC
322	GCT	GAA	AAC	ATG	TCT	TTA	TTA	ACT	CTG	AGA	AAC	AGC	AGC
323	GAA	AAC	ATG	TCT	TTA	GAA	GAC	CTG	AGA	AAC	AGC	AGC	CCA
324	AAC	ATG	TCT	TTA	GAA	ACT	TGG	AGA	AAC	AGC	AGC	CCA	GAA
325	ATG	TCT	TTA	GAA	ACT	CTG	TTC	AAC	AGC	AGC	CCA	GAA	GAC

326	TCT	TTA	GAA	ACT	CTG	AGA	TTA	AGC	AGC	CCA	GAA	GAC	CTC
327	TTA	GAA	ACT	CTG	AGA	AAC	GAC	AGC	CCA	GAA	GAC	CTC	TTT
328	GAA	ACT	CTG	AGA	AAC	AGC	GAC	CCA	GAA	GAC	CTC	TTT	GAT
329	ACT	CTG	AGA	AAC	AGC	AGC	TGG	GAA	GAC	CTC	TTT	GAT	GAG
330	CTG	AGA	AAC	AGC	AGC	CCA	TTA	GAC	CTC	TTT	GAT	GAG	ATT
331	AGA	AAC	AGC	AGC	CCA	GAA	TTA	CTC	TTT	GAT	GAG	ATT	CTC
332	AAC	AGC	AGC	CCA	GAA	GAC	TGG	TTT	GAT	GAG	ATT	CTC	GAC
333	AGC	AGC	CCA	GAA	GAC	CTC	TAT	GAT	GAG	ATT	CTC	GAC	GGT
334	AGC	CCA	GAA	GAC	CTC	TTT	TTA	GAG	ATT	CTC	GAC	GGT	ACC

From the modified sequence table, forward primers and reverse primers were designed as shown in Table 3-4.

Table 3 - 4. Forward and reverse primer of XECT mutants

M319C_F	5’- GAAAACTGTTCTTTAGAAACTCTGAGA -3’
M319C_R	5’- TAAAGAACAGTTTTCAGCTGAGATGTG -3’
S320D_F	5’- TTCTAAGTCCATGTTTTCAGCTGAGAT -3’
S320D_R	5’- AACATGGACTTAGAAACTCTGAGAAAC -3’
L321W_F	5’- ATGTCTTGGGAAACTCTGAGAAACAGC -3’
L321W_R	5’- AGTTTCCCAAGACATGTTTTCAGCTGA -3’
E322L_F	5’- TCTTTATTAACTCTGAGAAACAGCAGC -3’
E322L_R	5’- CAGAGTTAATAAAGACATGTTTTCAGC -3’
T323D_F	5’- TTAGAAGACCTGAGAAACAGCAGCCCA -3’

T323D_R	5’- TCTCAGGTCTTCTAAAGACATGTTTTC -3’
L324W_F	5’- GAAACTTGGAGAAACAGCAGCCCAGAA -3’
L324W_R	5’- GTTTCTCCAAGTTTCTAAAGACATGTT -3’
R325F_F	5’- ACTCTGTTCAACAGCAGCCCAGAAGAC -3’
R325F_R	5’- GCTGTTGAACAGAGTTTCTAAAGACAT -3’
N326L_F	5’- CTGAGATTAAGCAGCCCAGAAGACCTC -3’
N326L_R	5’- GCTGCTTAATCTCAGAGTTTCTAAAGA -3’
S327D_F	5’- AGAAACGACAGCCCAGAAGACCTCTTT -3’
S327D_R	5’- TGGGCTGTCGTTTCTCAGAGTTTCTAA -3’
S328D_F	5’- AACAGCGACCCAGAAGACCTCTTTGAT -3’
S328D_R	5’- TTCTGGGTCGCTGTTTCTCAGAGTTTC -3’
P329W_F	5’- AGCAGCTGGGAAGACCTCTTTGATGAC -3’
P329W_R	5’- GTCTTCCCAGCTGCTGTTTCTCAGAGT -3’
E330L_F	5’- AGCCCATTAGACCTCTTTGATGAGATT -3’
E330L_R	5’- GAGGTCTAATGGGCTGCTGTTTCTCAG -3’
D331L_F	5’- CCAGAATTACTCTTTGATGAGATTCTC -3’
D331L_R	5’- AAAGAGTAATTCTGGGCTGCTGTTTCT -3’
L332W_F	5’- GAAGACTGGTTTGATGAGATTCTCGAC -3’
L332W_R	5’- ATCAAACCAGTCTTCTGGGCTGCTGTT -3’
F333Y_F	5’- GACCTCTATGATGAGATTCTCGACGGT -3’
F333Y_R	5’- CTCATCATAGAGGTCTTCTGGGCTGCT -3’
D334L_F	5’- CTCTTTTTAGAGATTCTCGACGGTACC -3’
D334L_R	5’- AATCTCTAAAAAGAGGTCTTCTGGGCT -3’

3.2.5.3 Plasmid construction

Polymerase Chain Reaction **(**PCR) was performed using PrimeSTAR Max Premix (2X) [Kit Code R046A] with pEGFP-C1 vector containing wild type XRCC4 insert as the plasmid. PrimeSTAR Max Premix (1X), forward primer and reverse primer with a final concentration of 0.2 μM, plasmid concentration in the range of 10-100 pg/μl were mixed with deionized water in PCR tubes to make a final volume of 10 μl for each mutation sample, and then PCR tubes were placed inside the PCR Thermal cycler Dice (TaKaRa, Japan) under the condition shown in Table 3-5.

Table 3 - 5. Polymerase chain reaction condition.

Initialization step	98 ℃ for 3 min
Denaturation step	98 ℃ for 10 sec
Annealing step	55 ℃ for 15 sec
Elongation step	72 ℃ for 30 sec
Final elongation	72 ℃ for 6 min
Final hold	4 ℃ until use

After this step, PCR products for mutated XRCC4 are contained in the plasmid.

3.2.5.4 Lysogeny Broth (LB) plates

Lysogeny Broth or LB is a nutritionally rich medium for growing bacteria. 2.5% w/v of LB broth and 1.5% w/v of agarose in deionized water were mixed together and autoclaved at 121°C for 21 minutes. The mixture was left to cool down to around 40°C before the antibiotic kanamycin (final concentration: 50 μg/ml) was added. After that

LB medium was poured into the prepared plate (20 ml per plate). Avoid bubbles. Once solidified, the LB plates were kept in bacteria culture refrigerator at 4°C before use.

3.2.5.5 Transformation of E. coli (HIT-JM109) competent cell

Transformation is a process in which exogenous genetic material is introduced into a bacterial cell. Bacterial cells are considered as competent cells due to their capability of uptaking exogenous DNA from its surrounding through their cell membranes both naturally and artificially.

LB plates were pre-warmed at 37°C for 30 minutes. E. coli (HIT-JM109) was used as the competent cell in this study. Competent cells from -85°C deep freezer were thawed 30% only by dipping in room temperature water for 10 seconds. 20 µl aliquots were prepared. These steps should be handled on ice. After that, maximum of 10% v/v of each PCR product was added into aliquot of competent cells. The solution was placed on ice for 10 minutes. For higher efficiency, heat shock at 42°C which enhance the uptake of exogenous DNA into E. coli was performed for 1 minute followed by another 10 minutes on ice before the solution was plated onto LB plate, which was later incubated in 37°C incubator overnight.

3.2.5.6 Proliferation of competent cells

After one night, colonies were formed in the LB plate containing antibiotic (Kanamycin). Kanamycin was added to selectively exclude E. coli without the exogenous DNA of interest. pEGFP-C1 vector contains Kanamycin resistant gene. Therefore, E. coli with the inserted plasmid can grow in the presence of Kanamycin.

A single colony was picked up using pipette tip and placed in a 15 ml centrifuge tube containing 3 ml LB medium (2.5% w/v of LB broth powder in deionized water) supplemented with Kanamycin (final concentration 30 μg/ml), which was pre-autoclaved and kept at room temperature. Then the 15 ml centrifuge tube with a single colony was kept in shaker incubator at 37°C with 180 r/min overnight for E. coli to proliferate.

3.2.5.7 Bacterial freeze stock

After proliferation process, the recombinant DNA plasmid was amplified. One-third of the proliferated E. coli was prepared as freeze stock in case there are some problems with the present experiment. 900 μl of proliferated competent cells in LB medium were mixed with 100 μl of glycerol and stored using cryotube in -80°C deep freezer.

3.2.5.8 Elution of DNA

NucleoSpin Plasmid/Plasmid (NoLid) protocol was used to isolate high copy plasmid DNA from E. coli. Firstly, bacterial cells were cultivated and harvested. Then the cells were lyzed and their lysates were clarified. DNA was binded to the column. The silica membrane was washed and dried. After that, DNA was eluted. The concentration of the plasmid was measured using NanoDrop ND-1000 Spectrophotometer.

3.2.5.9 Insert check

Insert check was performed after polymerase chain reaction to check whether the insert of interest is present in the recombinant plasmid or not. PCR product with loading buffer was treated with restriction enzyme and loaded into electrophoresis gel containing 2.5% w/v of agarose in 0.5% TBE buffer, a solution containing a mixture of Tris base, boric acid and EDTA. The electrophoresis machine was run for 30 min at 100 V. Two bands can be observed where one of the bands represents pEGFP-C1 vector and another band represents the mutated XRCC4 insert.

3.2.5.10 Sequence check

Eluted DNA was sent for sequence check for accuracy of the mutation prior to transfecting into mammalian cells and establishing a stable clone. Sequence check sample was prepared containing 300-600 ng of plasmid and 6.4 pmol of universal primer in a final volume of 14 µl.

3.2.5.11 Transfection

Transfection is a process which plasmid DNA is introduced into mammalian cells. To examine the functionality of mutated XRCC4, plasmid containing normal and mutated XRCC4 cDNA was transfected into M10 cells through electroporation with Neon Transfection System (Invitrogen, Calsbad, CA, USA). Electroporation is a process by which an external electrical field is applied to increase the electrical conductivity and permeability of the cell plasma membrane. 10^6 cells per ml were transfected with 1 µg/ml of plasmid DNA. RPMI1640 medium supplemented with only

10% fetal bovine serum (FBS). After transfection was completed, solution was plated into a 6-well plate containing 2 ml of pre-warmed medium overnight.

After 24 hours of incubation, transfected cells were plated onto 0.17% w/v agarose plate containing RPMI1640 medium supplemented with 15% FBS, 1% Penicillin and streptomycin, 10 μM β-mercaptoethanol and G418 with final concentration of 0.8 mg/ml. Medium with agarose was autoclaved at 121°C for 21 minutes prior to plating process and warmed in a 42°C water bath. Cells were transferred from 6-well plate to 10-cm plate and incubated in cell culture incubator. Once colonies formed, they were picked up and cultured in complete culture medium and also kept as freeze stock.

3.3 RESULTS

3.3.1 NCBI database analysis of XECT domain

C-terminal region of all the species retrieved from NCBI database is shown in Figure 3-5, which showed a highly conserved C-terminal domain of XRCC4. Database of XRCC4 proteins can be seen in Appendix.

H.sapiens	301	PDSSLPETSKKEHISAENMSLETLRNSS-PEDLFDEI	336
P.paniscus	299	PDSSLPETSKKEHISAENMSLETLRNSS-PEDLFDEI	334
G.gorilla	299	PDSSLPETSKKEHISAENMSLETLRNSS-PEDLFDEI	334
P.troglodytes	299	PDSSLPETSKKEHISAENMSLETLRNSS-PEDLFDEI	334
N.leucogenys	299	PDSSLPETSKKEHISAENMSLETLRNSS-PEDLFDEI	334
P.abelii	299	PDSSLPETSKKEHISAENMSLETLRNSS-PEDLFDEI	334
P.anubis	301	PDSSLPETSKKEHISAENMSLETLRNSS-PEDLFDEI	336
M.mulatta	301	PDSSLPETSKKEHISAENMSLETLRNSS-PEDLFDEI	336
M.fascicularis	299	PDSSLPETSKKEHISAENMSLETLRNSS-PEDLFDEI	334
S.boliviensis	301	PDSSLPETLKKEHISAENMSLETLRNSS-PEDLFDEI	336
C.jacchus	299	PDSSLPETLKKEHISAENMSLETLRNSS-PEDLFDEI	334
O.orca	300	LDPPLPEMLKKDHSPAENMSLETLRNSS-PGDLFDEI	335
O.divergens	298	LDPSPPETSKKEHSSAENMSLETLRNSS-SEDLFDEI	333
O.garnettii	300	P--SLPATLKKEPISAESVSLETLRNSS-PEDLFDEI	333
E.caballus	300	HEPPLPEALRKEHSSAENMSLETLRNRS-PEDLFDEI	335
C.simum	300	P--PVPETLRKEHSSAENMSLETLRNSS-PEDLFDKI	333
O.aries	297	LDPPLPEMPKKDHGSAENMSLETLRNSS-PGDLFDEI	332
T.latirostris	298	LDPSLPQTLKKEHSSAENMSLETLRNTS-PEDLFDEI	333
C.familiaris	300	LDPPLPETSKKEHSSAENMSLETLRNSS-SEDLFDEI	335
B.taurus	298	LDPPLPEMPKKDHGPAENMSLETLRNSS-PGDLFDEI	333
M.furo	300	P--PLPETSKKEHSSAENMSLETLRNSS-SEDLFDEI	333
M.musculus	293	LASSLPQTLKEESTSAENMSLETLRNSS-PEDLFD	326
H.glaber	298	PDASQPEMSKKEHISVGNMSLETLRNSS-PEDLFDEI	333
C.porcellus	298	LDPARPEMSEKEHISAENTSLETVRISS-QGDLFDEI	333
S.araneus	297	LDTPLPETLEK-HSSDENLSLETLKNTS-SEDLFDEI	331
J.jaculus	293	LDPALPETLKEEPVSSENLSLETLRNSS-PEALFDDI	328
R.norvegicus	290	LGSSPPQTLKEEGTSAAKMSLETLRNSS-PEDLFD	323
S.harrisii	300	PESSQLQSSSKEPFSSENMSLETLKNSS-PEDLFDDM	335
E.telfairi	315	P--SVPQMLKKEGSSTENMSLETLRNTN-PEDLFDEI	348
M.domestica	300	EDPSPLQSSSKESISSENLSLETLKNSS-PEDLFEDI	335
G.gallus	300	PDLSSQKSSGKH--SPDVMSLETLENTCEPEDLFDDI	334
A.platyrhynchos	291	PDPASEKTSGKH--SPDVMSLETLENTCEPEDLFDDI	325
X.laevis	329	P---APAQSVGKTFSTEGTSSQTLKNTPDPDDLFSDI	362
X.tropicalis	304	P---VPAKAVGTTLSTEGTSSQTLINTPDPDDLFSDI	337
D.rerio	323	EETKA-ATSRTSSVPVKPAN--TAANLD-PDELFDDI	357

Figure 3 - 5. Comparison of C-terminal domain of all the species (NCBI database).

3.3.2 Generation of serial mutants of XECT domain

pEGFP-C1 plasmid containing wild type XRCC4, pEGFP-C1 plasmid containing mutated XRCC4 were treated with two restriction enzymes EcoRI and KpnI and run electrophoresis. The result in Figure 3-6 showed two bands: the upper one lied slightly above 3 kbp marker corresponds to the pEGFP-C1 plasmid, which has the molecular mass of 4.731 kbp, and the lower one which lied around 1 kbp marker corresponded to the XRCC4 inserts. Normal human XRCC4 has the molecular mass of 1.694 kbp. These results confirmed that the mutated constructs were contained in the constructed plasmids.

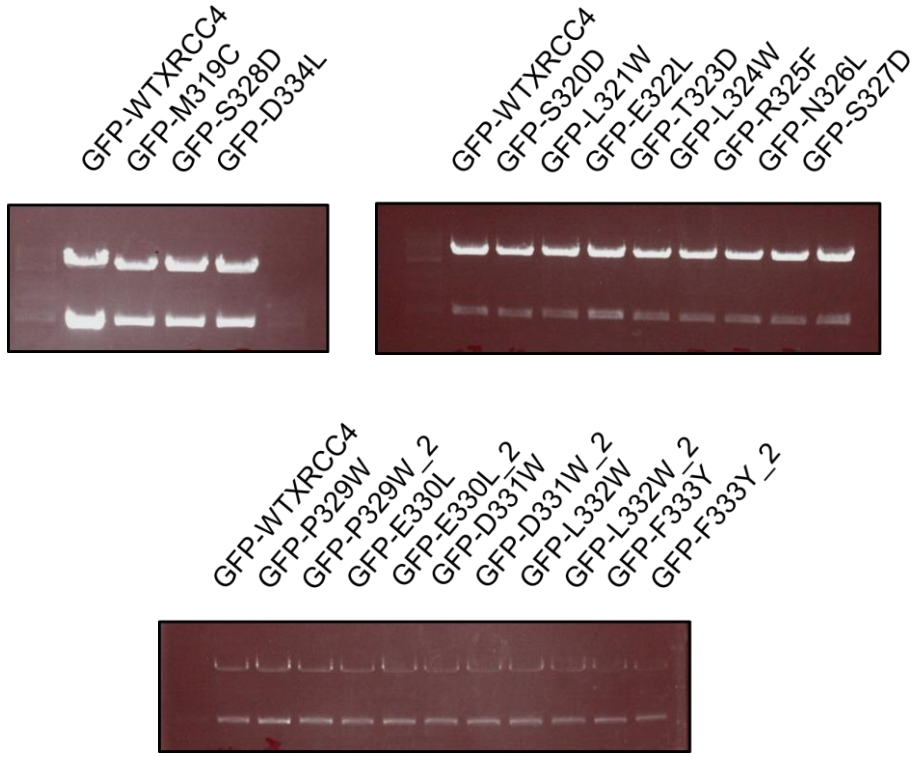

Figure 3 - 6. Insert check results of different mutated plasmid constructs with EcoRI and KpnI restriction enzymes.

XRCC4 sequence checks with nucleotide blast program comparing the mutated nucleotide sequence to the original nucleotide sequence of pEGFP-C1 with wild type human XRCC4 cDNA showed the correct mutation position in each construct. Mismatched mutation or frame shift constructs must be redo again until correct mutation was obtained. The results contained a common mismatch at nucleotide 636 where alanine (A) was mutated to glutamine (G), nevertheless GAA or GAG corresponded to the same amino acid which is Glutamic acid (Glu). This would not interrupt the protein expression of XRCC4.

Constructs of wild-type XRCC4 and mutated XRCC4 fused with GFP-tag vector (pEGFP_C1) were transfected into M10 cells via Neon transfection. The successful mutants were observed under fluorescent microscope and evaluated using western blotting with XRCC4 antibody or GFP antibody. Western blotting results were shown in Figure 3-7.

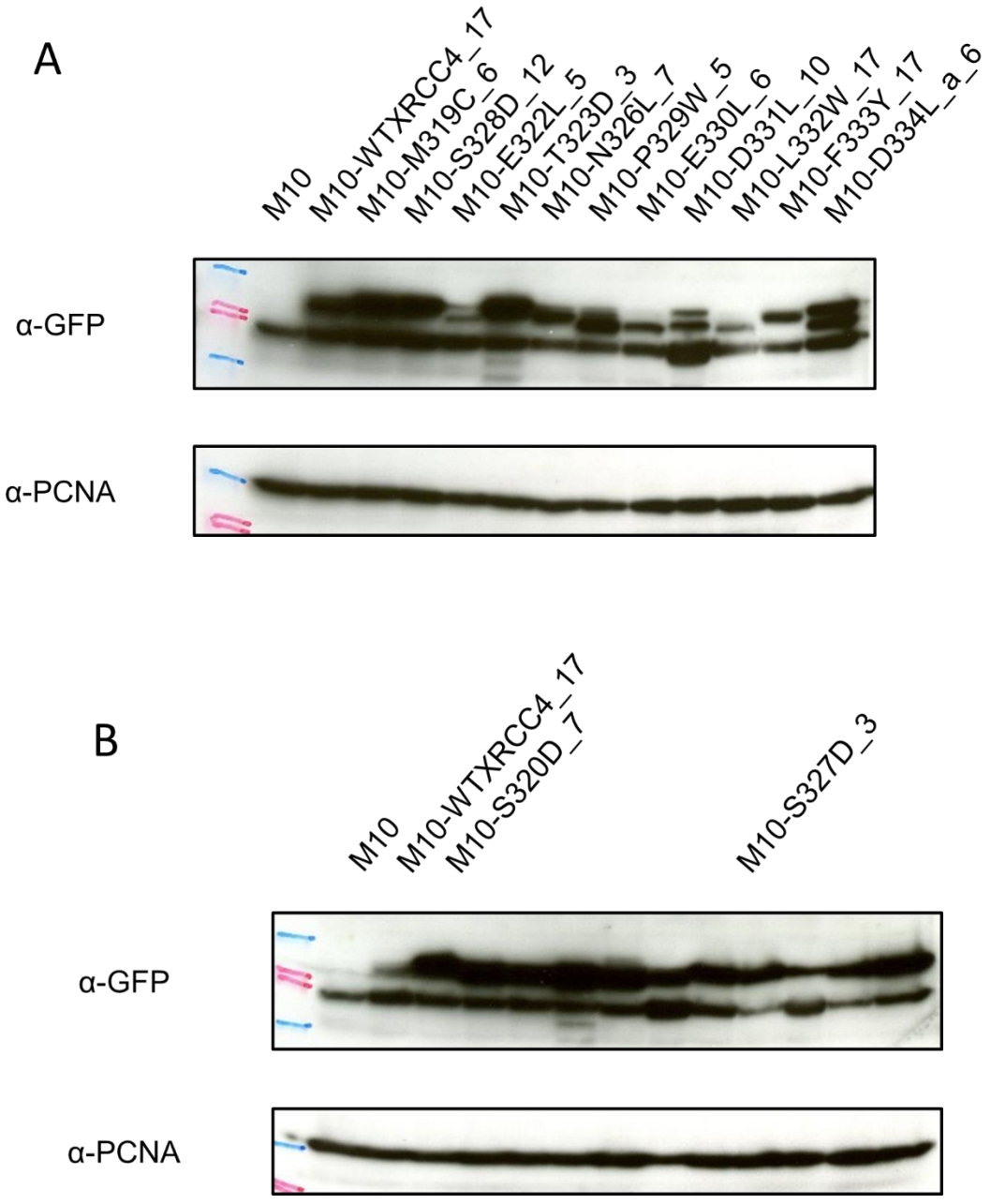
A
M10
M10-WTXRCC4_17
M10-M319C_6
M10-S328D_12
M10-E322L_5
M10-T323D_3
M10-N326L_7
M10-P329W_5
M10-E330L_6
M10-D331L_10
M10-L332W_17
M10-F333Y_17
M10-D334L_a_6
α-GFP
α-PCNA
B
M10
M10-WTXRCC4_17
M10-S320D_7
M10-S327D_3
α-GFP
α-PCNA

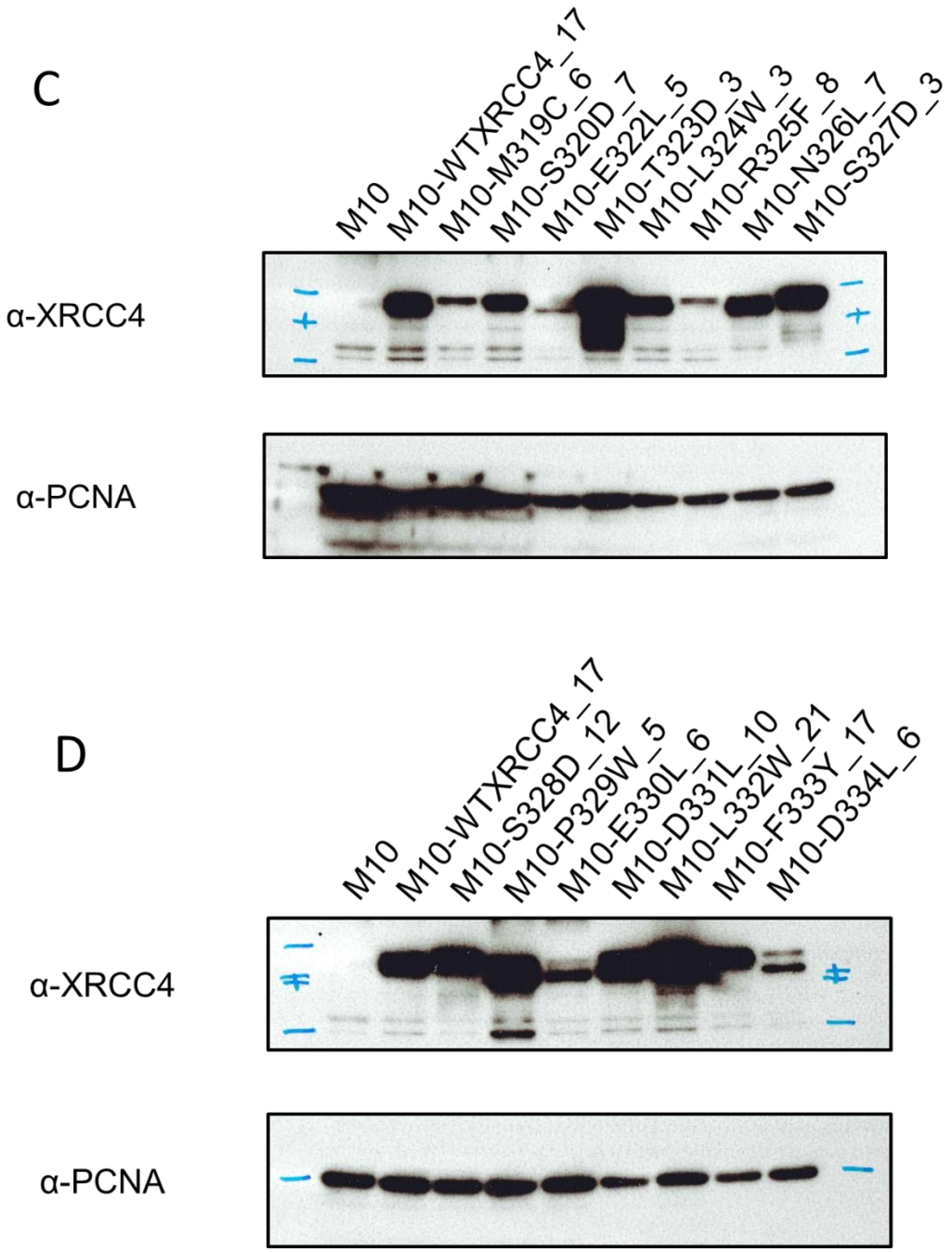

Figure 3 - 7. Western blotting result of successfully transfected XECT mutants. a.) and b.) immunoblotted with GFP antibody and c.) and d.) immunoblotted with XRCC4 antibody.

3.3.3 Analysis of radiosensitivity of XECT mutants

Fifteen XRCC4 C-terminal mutants, which are highly conserved across vertebrate species, were successfully established by systematically modified their charge, side chain and polarity. Mutated XRCC4 cDNAs were used to transform M10 cells, harboring inactivation mutation in XRCC4 gene. We evaluated the functionality of mutated XRCC4 as compared to wild-type XRCC4 (WT) expressing normal function of XRCC4 protein, in terms of clonogenic survival of transformants after γ-irradiation.

As a result shown in Figure 3-8, M10 cells showed high radiosensitivity (SF2 ≒ 0.1), whereas transformants with wild-type XRCC4 (WT) restored normal level of radiosensitivity (SF2 ≒ 0.6 and 0.65). The other 13 mutants showed similar radiosensitivity to WT, 2 mutants, *i.e.*, R325F and N326L, showed significantly elevated radiosensitivity as compared to WT. These results indicated that XRCC4 C-terminal domain contained regions, *i.e.*, around amino acids mutated in R325F and N326L, essential for DSB repair.

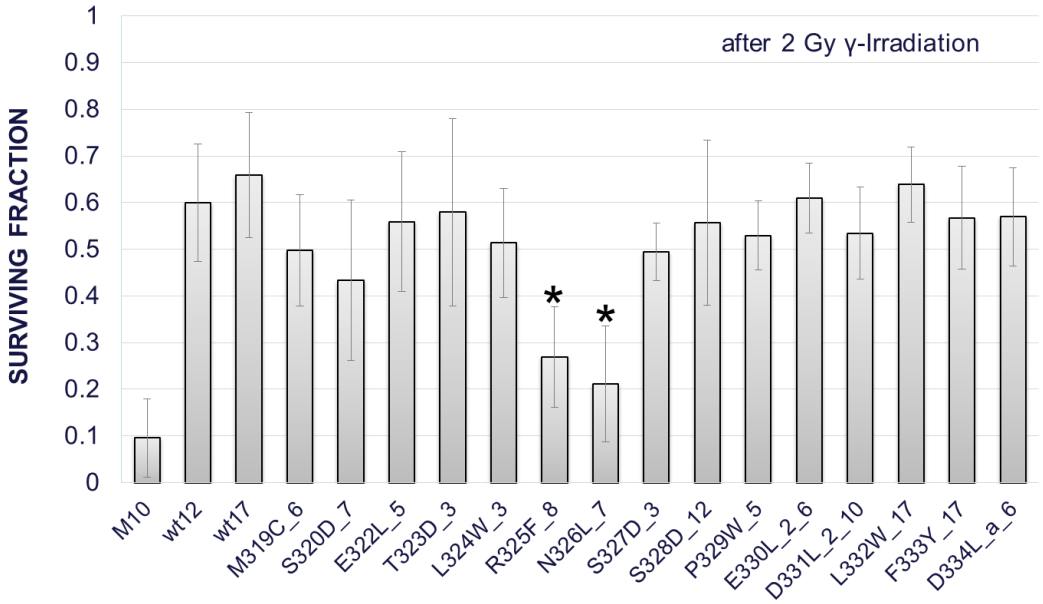

Figure 3 - 8. Colony formation assay result of M10 cells transfected with wild-type XRCC4 (WT) and mutated XRCC4 after 2 Gy of γ-irradiation. Asterisk (*) represents statistically significance of surviving fraction when compared to normal XRCC4's surviving fraction ($p<0.025$). Statistical analysis used in this analysis is the two-tailed t-test distribution. Error bars are the standard deviation of the samples. At least three experiments were conducted.

3.4 DISCUSSION

In this chapter, series of XRCC4 mutants in the XECT domain (XECT mutants) were systematically constructed by changing their polarity, charge or side chain, and stable transformants were successfully established for further functional analysis of XECT domain in details. After the analysis of the radiosensitivity of XECT mutants through the colony formation assay after 2 Gy irradiation, two of the XECT mutants were found to be significantly radiosensitive (M10-R325F and M10-N326L) compared to the wild-type XRCC4 (M10-XRCC4). However, it could not be excluded that the radiosensitivity of M10-R325F was due to the low XRCC4 protein expression. Further analysis of the radiosensitivity of M10-N326L was performed in the next section.

CHAPTER 4

ANALYSES OF XRCC4 N326 IN DNA REPAIR

4.1 INTRODUCTION

In this chapter, the radiosensitive mutants (R325F and N326L) were further analyzed for their radiosensitivity by analyzing their nuclear localization function.

To search for the role of N326 in DNA DSB repair, N326 was further mutated from asparagine (polar uncharged) into alanine (hydrophobic), aspartic acid (polar charged), and glutamine (polar uncharged) (Figure 4-1).

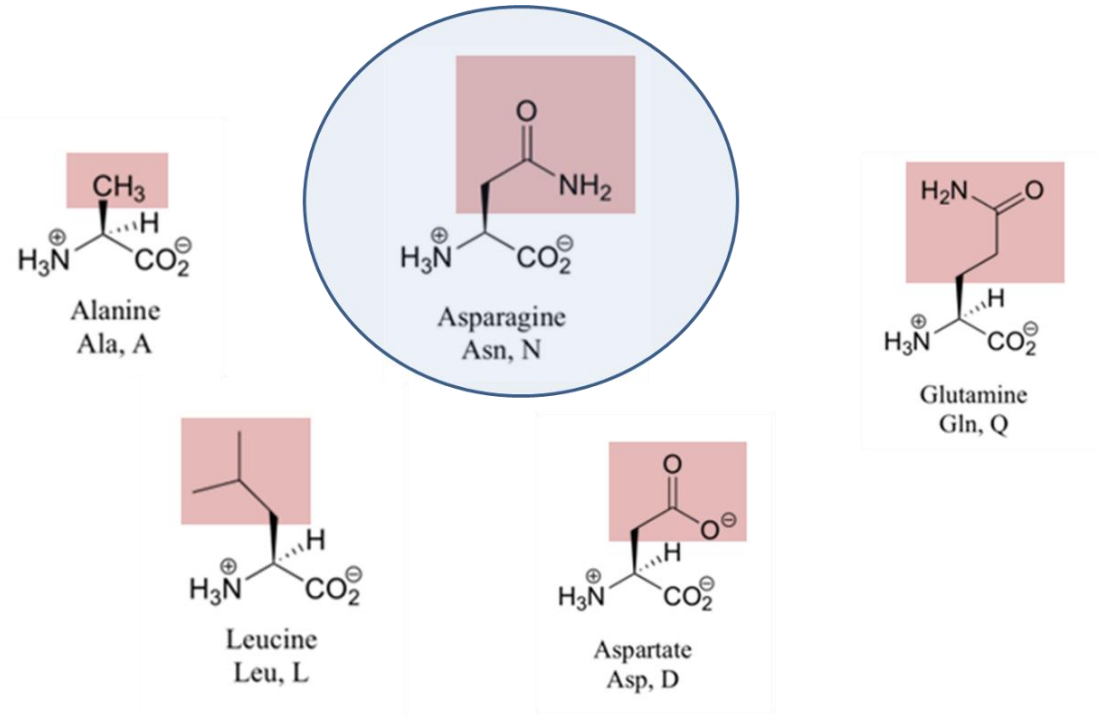

Figure 4 - 1. Amino acid structure with red highlight for the side chain of Alanine, Asparagine, Lysine, Leucine and Aspartate and Glutamine.

4.2 MATERIALS AND METHODS

4.2.1 Cell culture

In this chapter, M10 cells and HeLa cells were used.

M10 cells were cultured in RPMI1640 medium supplemented with 10% v/v fetal bovine serum (FBS) or calf bovine serum (CBS), 1% v/v of penicillin-streptomycin mixed solution (5,000 U/ml penicillin and 5,000 μg/ml streptomycin) as antibiotics and 10 μM of β-mercaptoethanol.

Human cervical carcinoma cell line HeLa was cultured in DMEM/Ham's F-12 medium supplemented with 10% v/v FBS, 1% v/v of penicillin-streptomycin mixed solution and 10 μM of β-mercaptoethanol at 37 °C in humidified atmosphere containing 5% CO_2. Cells were cultured in 25 cm^2 or 75 cm^2 culture flasks with 5 ml or 20 ml of complete culture media, respectively, in a humidified 5% CO_2 at 37°C.

FBS and CBS were purchased from Hyclone (Logan, UT, USA). RPMI1640 medium and other agents were purchased from Nacalai Tesque (Kyoto, Japan). Addition of small amount of penicillin and streptomycin as antibiotics are used to prevent bacterial contamination of cell cultures due to their effective action against gram-positive and gram-negative bacteria, respectively, which do not affect the mammalian cell culture.

4.2.2 Transfection

For M10 cells, plasmids were transfected using Neon Transfection system (Invitrogen; Carlsbad, CA, USA). Two days after transfection, cells were plated in RPMI1640 medium supplemented with 15% v/v FBS, 100 units/ml penicillin, 100

μg/ml streptomycin, 10 μM β-mercaptoethanol and 0.2% agarose (Difco). Two weeks after plating, visible colonies were picked up and cultured in G418 containing complete medium for drug selection. After several passages, the stable transformants of different mutated XRCC4 constructs were established.

For HeLa cells, plasmids were transfected using Lipofectamine 2000 Reagent (Invitrogen). To knockdown the endogenous XRCC4 in HeLa cells, small interfering RNA (siRNA) targeting 3'-untranslated region (UTR) was transfected 24 hr prior to the transfection of the plasmid. The sequences of RNA duplex were 5'- CUA UGU UUU CUA UUC AUU UdCdT -3' and 5'- AAA UGA AUA GAA AAC AUA GdTdC -3', where "d" indicates deoxyribonucleotide. Oligonucleotides were synthesized by Japan Bioservice (Saitama, Japan).

4.2.3 Analysis of nuclear localization

Fluorescence of EGFP was observed with an inverted fluorescence microscope, IX71 (Olympus; Tokyo, Japan). The nucleus of transfected cells was stained with 4',6-diamidino-2-phenylindole (DAPI).

4.2.4 Treatment with Leptomycin B

Leptomycin B was dissolved in 99.5% ethanol at the concentration of 1 or 50 mg/ml for stock and kept at -20ºC. Leptomycin B was added to the culture medium at the final concentration of 1 to 100 ng/ml, as indicated, two hours prior to irradiation.

4.2.5 Generation of XRCC4 N326 mutants

The method used to create N326 mutants was similar to the method used to create series of XECT mutants, which was explained in section 3.2.2 (Chapter 3).

The primer sequences for N326 mutants were shown in Table 4-1.

Table 4 - 1. Forward and reverse primer of N326 mutants.

N326A_F	5'- CTGAGAGCCAGCAGCCCAGAAGACCTC -3'
N326A_R	5'- GCTGCTGGCTCTCAGAGTTTCTAAAGA -3'
N326D_F	5'- CTGAGAGACAGCAGCCCAGAAGACCTC -3'
N326D_R	5'- GCTGCTGTCTCTCAGAGTTTCTAAAGA -3'
N326Q_F	5'- CTGAGACAAAGCAGCCCAGAAGACCTC -3'
N326Q_R	5'- GCTGCTTTGTCTCAGAGTTTCTAAAGA -3'

4.2.6 Immunoprecipitation

Immunoprecipitation is a technique to precipitate the target protein from different proteins existing in the cell lysate by using antibody-antigen binding with antibody immobilized to a solid substrate. There are two types of immunoprecipitation: direct and indirect methods. Direct method allows the binding of antibody and antigen to occur first before binding of antibody to the solid substrate. However, due to the low protein concentration or weak protein-antibody interaction, indirect method is preferred. In an indirect method, antibody to the specific protein of interest is immobilized on the solid substrate before allowing the complex to bind the protein.

In this study, indirect immunoprecipitation was used. Firstly, the conjugation of antibody to the solid substrate, such as agarose was done prior to binding to target protein. The antibody used can be target to protein itself or to tag protein, such as FLAG, green fluorescent protein (GFP), or Glutathione-S-Transferase (GST). Secondly, cells were lysed with lysis buffer including phosphatse inhibitors and protease inhibitors. Thirdly, the antibody-binded agarose solution was mixed with the cell lysate overnight. Lastly, protein-antibody-agarose was precipitated, and protein was eluted out by peptide elution or acid elution method. Samples were further analyzed with western blotting.

Two kinds of immunoprecipitation were conducted. First is the chicken XRCC4 immunoprecipitation (IP-chXRCC4). First step, chicken XRCC4 IgY antibody was conjugated with NHS-activated sepharose. XRCC4 antibody of 50 µg was dissolved in coupling solution (0.2M NaHCO3, 0.5M NaCl (pH 8.3)). Next, 100 µl of NHS activated sepharose was washed with cold 1 mM HCl for three times prior to mixing with the antibody in coupling solution and keep in refrigerator for overnight. After that, 1 ml of 0.5 M ethanolamine, 0.5 M NaCl (pH 8.3) for 2 hrs 30 min at room temperature to block unbind regions. Then the solution was centrifuged at 3000 rpm for 1 min at 4 °C. The pellet was washed alternatively with 1 ml of Deactivation buffer A (0.1 M Tris HCl (pH 8.9)) and Deactivation buffer B (0.1 M acetate buffer, 0.5 M NaCl (pH 4.5)) for 3-6 times. Cells were lysed with lysis buffer (50 mM Tris-HCl (pH 7.6), 150 mM NaCl, 0.5% TritonX100) containing 1% phosphatase inhibitors and 1% protease inhibitors for 30 min on ice. The lysis buffer was used in a ratio of 1 ml per 10 million cells. Next, the solution was centrifuged at 15,000 rpm for 1 minutes to collect the supernatant. The supernatant was mixed with chicken XRCC4 antibody conjugated

NHS-activated Sepharose and rotated in refrigerator for overnight. The following day, the solution was centrifuged for 1 min at 10,000 rpm. The supernatant was discarded. The pellet was washed three times with 1 ml of lysis buffer. Proteins were eluted using acidic elution protocol by adding 60 µl of 0.2 M Glycine-HCl (pH 2.8) and kept at 4 °C for 10 min. Then the solution was centrifuged at 10,000 rpm for 1 min. The supernatant was collected and neutralized using 6.25 µl of 0.2 M Tris HCl (pH 8.4). After that, sample buffer of 70 µl was added. The solution was heated at 100 °C for 10 min and centrifuged at 15,000 rpm for 1 min. Then the solution was collected for analysis with western blotting.

In the case of FLAG-tag immunoprecipitation, cells were lysed with lysis buffer and the supernatant was collected to bind with 20 µl of anti-flag M2 affinity gel (SIGMA) in 4 °C for overnight. Then, the solution was centrifuged at 10,000 rpm for 1 min at 4 °C and pellet was washed with lysis buffer for three times. Then sample buffer was added. The solution was heated at 100 °C for 10 min and centrifuged at 15,000 rpm for 1 min. Last, the solution was collected for analysis with western blotting.

4.2.7 Immunofluorescence

Immunofluorescence is one of the immunostaining technique, which utilized the specific binding of antibodies to antigens to target fluorescent dyes to the molecules of interest inside the cells. This technique allows the visualization of the subcellular protein localization through observation under the microscope. It can be used to observe protein responsible for DNA damages. There are two types of immunofluorescence technique: primary (direct) and secondary (indirect). Direct immunofluorescence utilizes single or primary antibody attached to the fluorescent dye (fluorophore). Once

the antibody binds to the target molecule, its localization can be observed directly under the fluorescent microscope. However, indirect immunofluorescence utilized two antibodies: primary and secondary antibody. Primary antibody first binds the target molecule, then secondary antibody attached to fluorophore recognizes and binds the primary antibody. The second technique although time consuming, but it is more flexible because secondary antibody with fluorophore can be used to recognize various primary antibodies of interest. In this study, the second technique was utilized.

For suspension cells like M10 cells, cell preparation was needed. First of all, cell sample was attached to glass slide by loading into the plastic tube inside a vacuum chamber slowly to avoid overflow of sample. The loaded chamber was centrifuged for 1200 rpm for 5 min at room temperature. After that filter paper was discarded and liquid blocker lines were drawn on the glass slide. The sample was fixed with 4% Paraformaldehyde phosphate buffer solution and incubated for 30 minutes. After 30 minutes, 4% Paraformaldehyde was removed and washing buffer (PBS) was added. The sample was dehydrated with 70% Ethanol for 10 minutes and washed one more time with PBS. Blocking buffer (1X PBS/0.5% Triton X-100/5% BSA) was added and incubated overnight at 4 °C.

The process was continued the next day. Blocking buffer was removed from the sample. The sample was incubated with primary antibody for 90 minutes at room temperature. Before proceeding on to the secondary antibody incubation and after the antibody incubation, the sample was washed with PBST (PBS/0.05% Tween 20) twice. The sample was incubated in secondary antibody for 45-60 min at room temperature. After washing, the sample was now stained with DAPI staining solution for 20 minutes before observing under fluorescent microscope.

For attached cells like HeLa cells, cells were cultured in glass bottom dish. After that, the sample was proceeded to fixation with 4% Paraformaldehyde and antibody binding as previously stated in suspension cell.

4.3 RESULTS

4.3.1 Nuclear localization function of radiosensitive mutants

Further study was done to elucidate the mechanism behind the radiosensitivity of R325F and N326L. Firstly, endogenous XRCC4 was knocked down in HeLa cells followed by transfection of mutated XRCC4 plasmid. Live cell imaging of HeLa cells transfected with mutated XRCC4 plasmid revealed the defectiveness in the localization of GFP-tagged mutated XRCC4 (HeLa_si+N326L) in the nucleus as compared to HeLa cells transfected with empty pEGFP-C1 vector (HeLa_si+GFP) and wild-type XRCC4 (HeLa_si+WTXRCC4) (Figure 4-3). However, live cell imaging of HeLa cells transfected with R325F plasmid did not revealed the defectiveness in the localization of GFP-tagged protein in the nucleus (Figure 4-2).

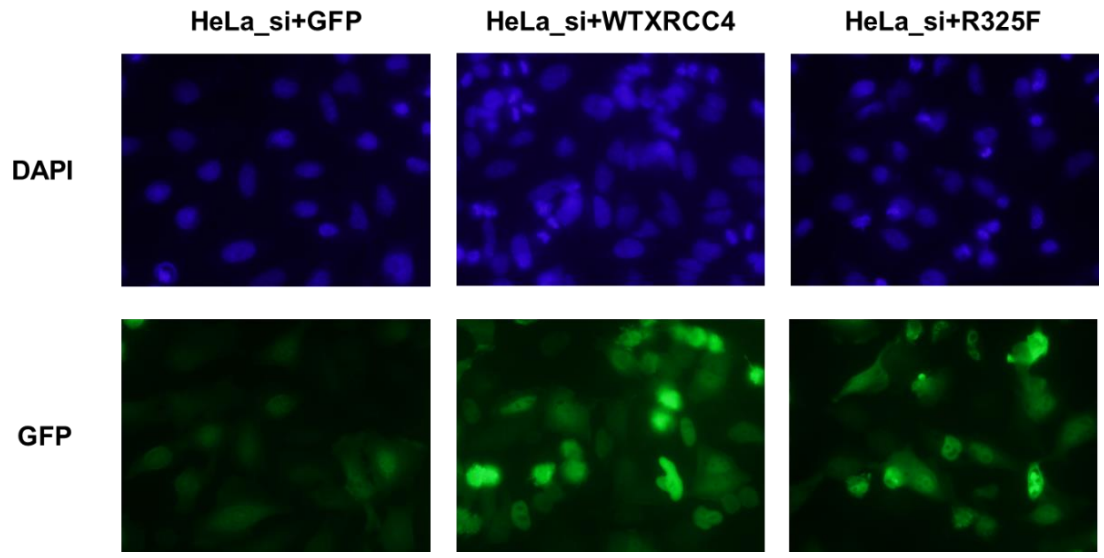

Figure 4 - 2. Normal function of nuclear localization signal in HeLa cells transfected with empty GFP vector, wild-type XRCC4 (WTXRCC4) and R325F mutant with siRNA treatment.

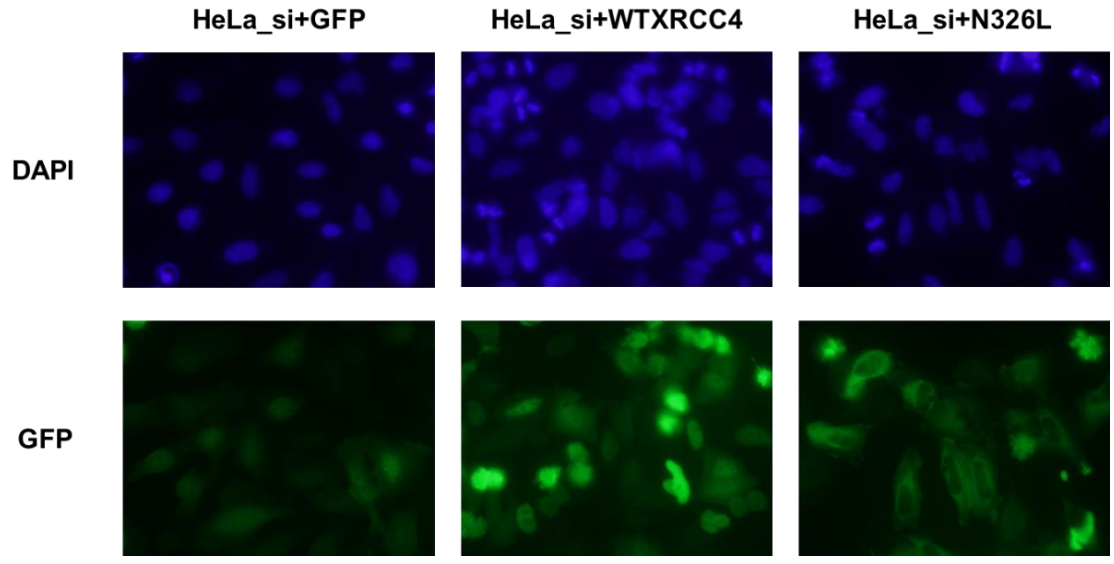

Figure 4 - 3. Defective in nuclear localization function of mutated XRCC4 (N326L) in HeLa cells via live-cell imaging with siRNA treatment.

To explore the effect of endogenous XRCC4 in dimerization with exogenous XRCC4 and recruit them into the nucleus, GFP-tagged mutated XRCC4 was transfected into HeLa cells and observed under fluorescent microscope. As a result, HeLa cells transfected with N326L also showed similar result as HeLa cells co-transfected with XRCC4 siRNA and GFP-tagged mutated XRCC4 (Figure 4-4).

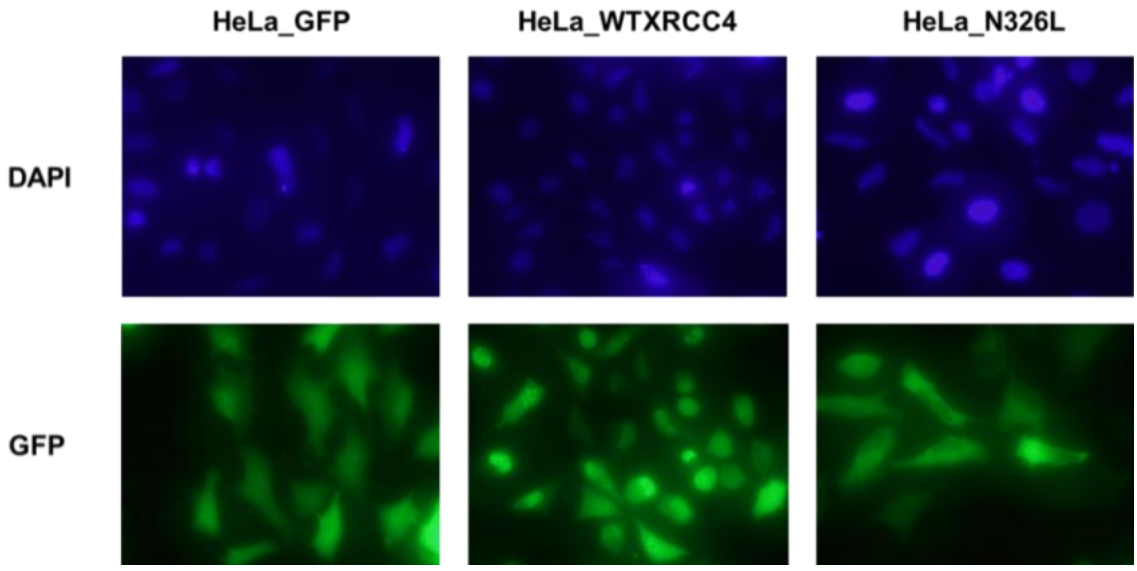

Figure 4 - 4. Defective in nuclear localization function of mutated XRCC4 (N326L) in HeLa cells via live-cell imaging without siRNA treatment.

4.3.2 Analyses of the recruitment of XRCC4 N326L mutant to DNA DSB

To check whether the mislocalization of XRCC4 N326L in the cytoplasm was due to the lost in ability to localize in the nucleus and DNA DSB site, chromatin binding study was performed in both M10 cells and HeLa cells.

4.3.3 Analysis of the interaction between DNA ligase IV and XRCC4 N326L mutant

XRCC4 and DNA ligase IV exist in tight complex and work collaboratively to join the broken DNA DSB ends in non-homologous end joining. Even though N326L is not located in the DNA ligase IV binding domain with XRCC4. Interruption of DNA ligase IV function was suspected due to the radiosensitivity of M10_N326L mutant. Leptomycin B reconstitute the radiosensitivity of M10_N326L to a certain extent but not equivalent to the wild-type XRCC4. The detection of DNA ligase IV with Ligase IV antibody is difficult to detect in M10 cells lacking XRCC4. This might be due to the destabilization of DNA ligase IV in the absence of XRCC4. Therefore, the interaction between DNA ligase IV and XRCC4 N326L mutant was studied in HeLa cell. HeLa cell contains both endogeneous XRCC4 and endogeneous DNA ligase IV. However, to clearly observe the interaction with exogeneous wild-type XRCC4 (WT) and exogeneous mutated XRCC4 N326L (N326L), both XRCC4 and DNA ligase IV were transfected into HeLa cells.

4.3.4 Nuclear localization function of N326L after treatment with nuclear export inhibitor, Leptomycin B

XRCC4 contains nuclear localization signal (NLS), however N326L was observed to be localized in the cytoplasm. Several studies about nuclear export signal (NES) had lead us to one of the nuclear export signal recognized by exportin1, CRM1, which is called leucine rich nuclear export signal (LR-NES). We hypothesized that mutation of N326 into leucine may mimic the nuclear export signal consensus (Figure

4-10). High leucine-rich region conferred nuclear export signal consensus (Kutay and Guttinger, 2005; Dong *et al,* 2009).

To clarify this hypothesis, a major nuclear export pathway through CRM1/exportin1 was blocked by treatment with Leptomycin B, a nuclear export inhibitor of CRM1. As a result, treatment with Leptomycin B (final concentration of 10 ng/ml) for two hours could clearly concentrate GFP-tagged mutated XRCC4 protein in the nucleus (nucleus > cytoplasm) (Figure 4-11) (Wanotayan *et al.,* 2015).

Protein	NES sequence	
HIV-1 Rev	L-PPL-ERLTL	
MVM NS2	MTKKF-GTLTI	
PKIα	LALKL-AGLDI	
PKIβ	LPLKLEA-LAV	
MAPKK	LQKKL-EELEL	
NMD3	LAEML-EDLHI	
An3	LDQQF-AGLDL	
IκBα	MVKEL-QEIRL	
Cyclin B1	LCQAF-SDVIL	
TFIIIA	L-PVL-ENLTL	
NES consensus:	$\Phi x_{2-3}\Phi x_{2-3}\Phi x\Phi$	
		NE localization
XRCC4 WT	M-S-L-ETLRN	-
XRCC4 N326L	M-S-L-ETLRL	+

XRCC4 NES: $\Phi x\Phi x_2\Phi x\Phi$

Figure 4 - 5. Leucine rich nuclear export signal consensus of different proteins compared with XRCC4 WT and XRCC4 N326L sequence (Φ: L,I,V,F,M; x: any other amino acids).

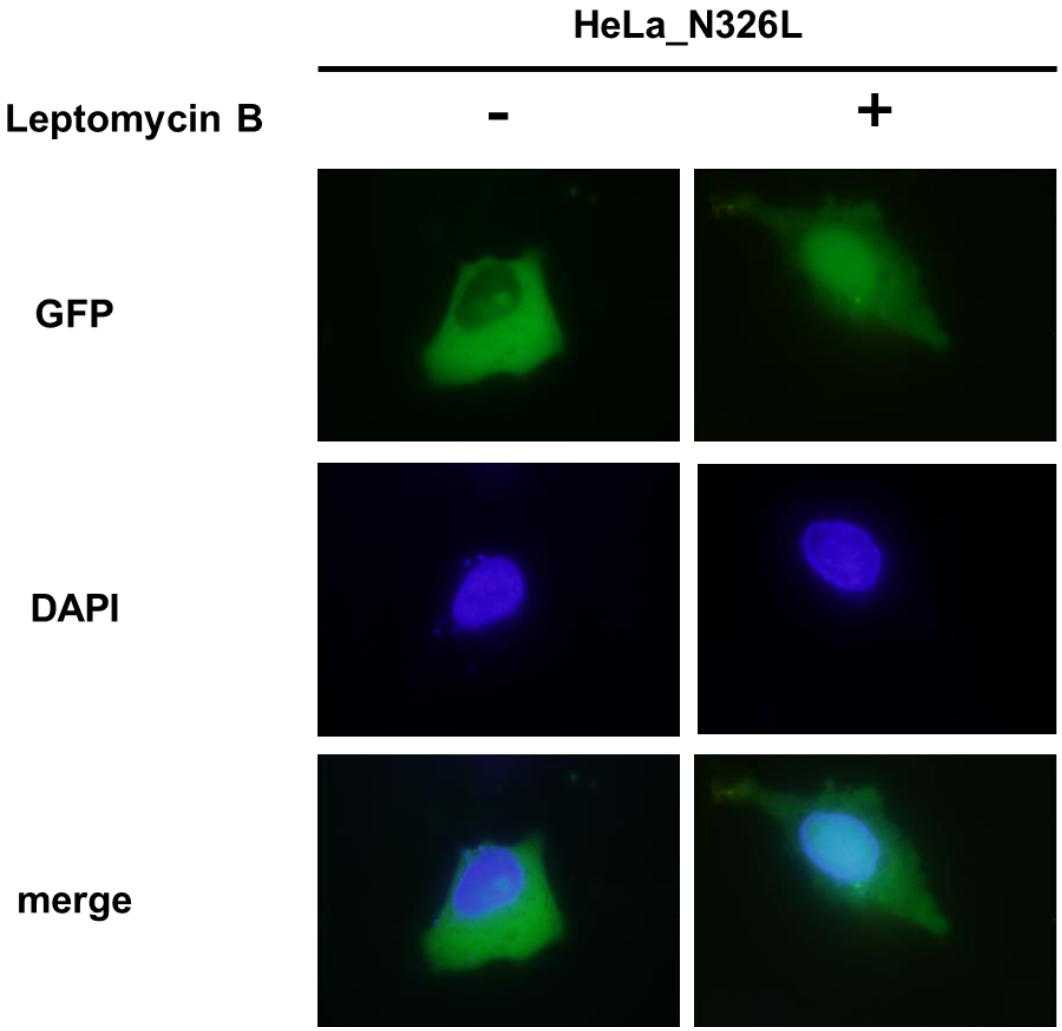

Figure 4 - 6. Live cell imaging of HeLa cells transfected with mutated XRCC4 N326L plasmid with and without treatment with 10 ng/ml of nuclear export inhibitor, Leptomycin B showed lack of nuclear localization and restored nuclear localization, respectively. (merge: GFP and DAPI; N:nucleus; C:cytoplasm)

4.3.5 Nuclear localization function of other XECT mutants into leucine

Therefore, other amino acids in the XECT region which were mutated into leucine, E322L, E330L, D331L and D334L, were investigated for their nuclear localization function. Nevertheless, none of the mutated XRCC4 showed lack of nuclear localization function (Figure 4-12).

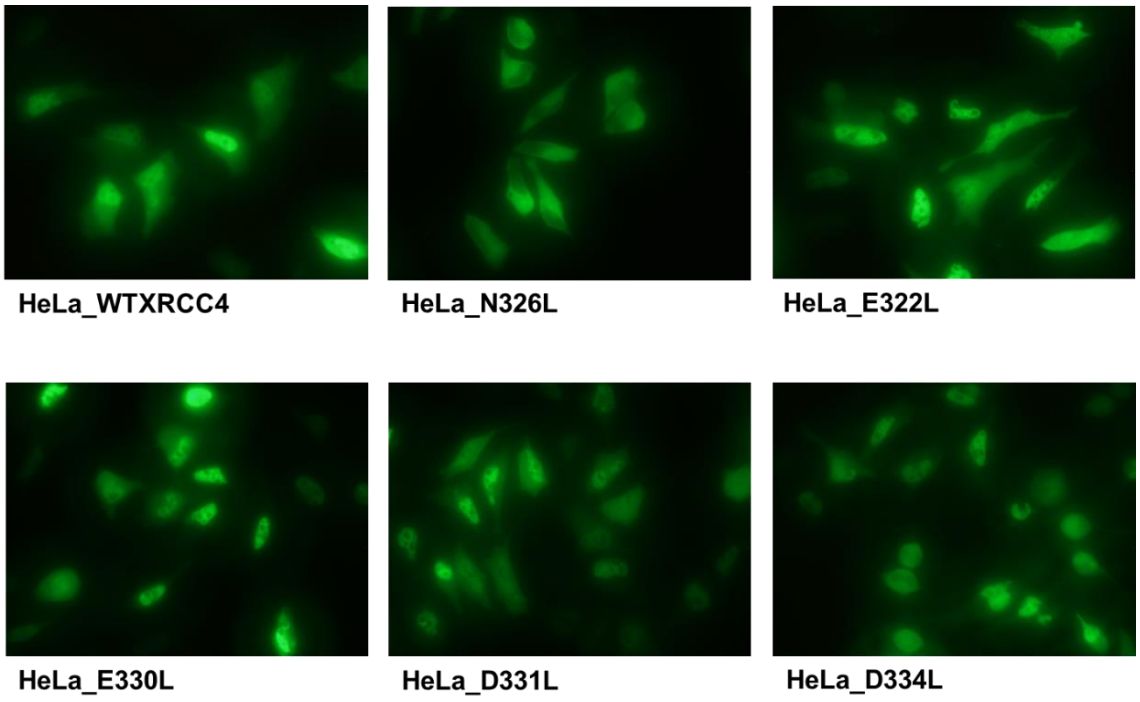

Figure 4 - 7. Defective in nuclear localization function of mutated XRCC4 N326L in HeLa cells via live-cell imaging compared to wild-type XRCC4 and other C-terminal mutation to leucine (E322L, E330L, D331L, D334L).

4.3.6 Importance of XRCC4 N326L nuclear localization in DNA repair

Next, the role of Leptomycin B in the DNA repair ability of M10-N326L was studied by assessing its radiosensitivity after ionizing radiation. Cells were incubated with Leptomycin B of various concentrations for two hours prior to irradiation. As a result, treatment of M10-N326L with 10 ng/ml of Leptomycin B showed the maximum surviving fraction of N326L (Figure 4-13).

The effect of Leptomycin B on M10 cells transfected with empty vector and wild-type XRCC4 (M10-GFP and M10-WTXRCC4, respectively) were also examined. Leptomycin B of a concentration of 10 ng/ml was used to treat M10-GFP (negative control) and M10-WTXRCC4 (positive control). Enhancement of cell killing was observed in M10-GFP and M10-WTXRCC4 (Figure 4-14). This result corresponded with earlier result of Sasaki *et al,* (1992) that Leptomycin B enhanced cell killing in normal cells (Wanotayan *et al.,* 2015). However, the increase in survival fraction of M10-N326L after treatment with Leptomycin B was still insufficient for N326L to function like wild-type XRCC4.

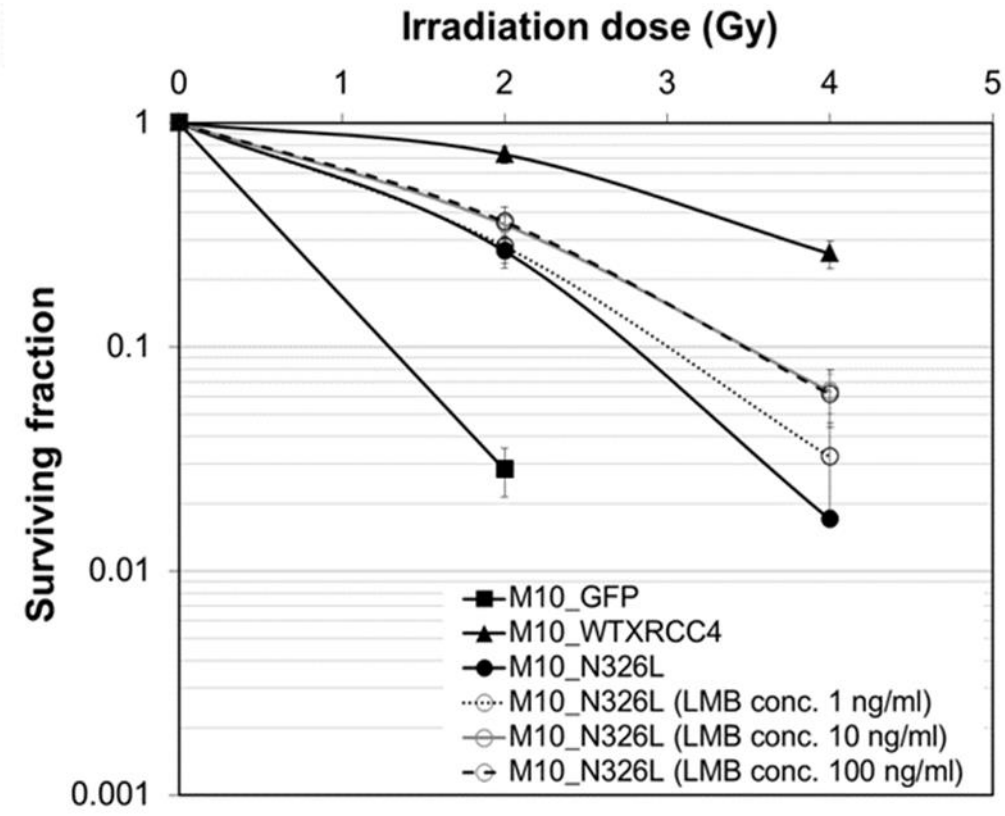

Figure 4 - 8. Surviving fraction of mutated XRCC4 (M10_N326L) treated with various doses of Leptomycin B (1 ng/ml, 10 ng/ml, 100 ng/ml).

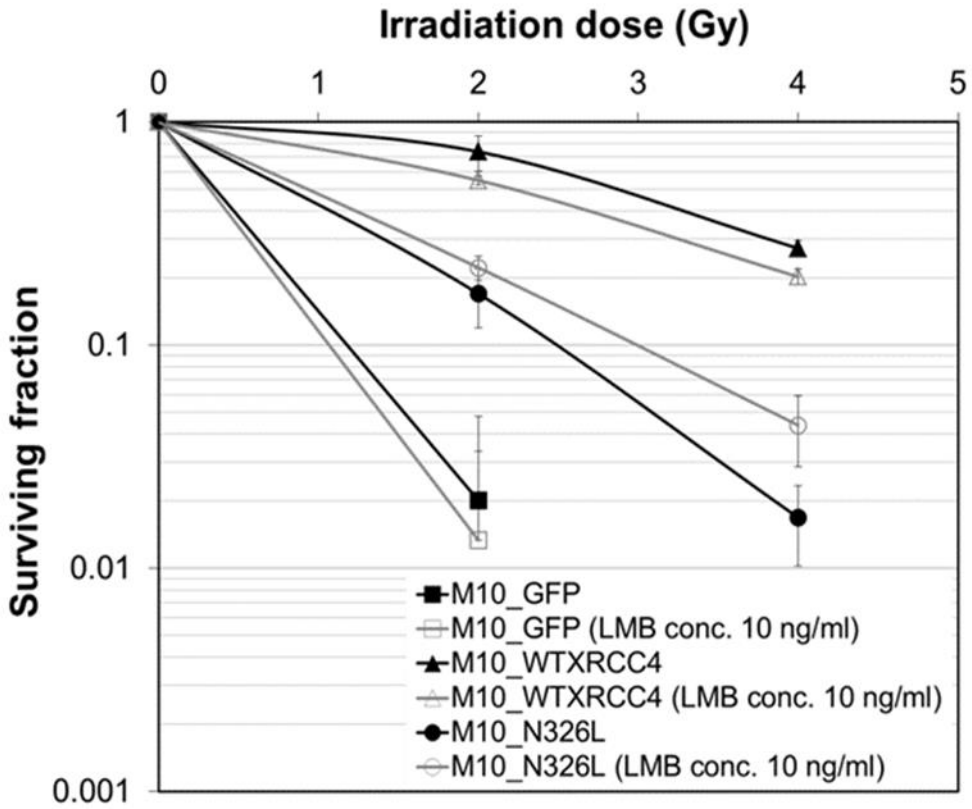

Figure 4 - 9. Surviving fraction of M10 cells transfected with empty vector (M10_GFP), wild-type XRCC4 (M10_WTXRCC4) and mutated XRCC4 (M10_N326L) treated with 10 ng/ml of Leptomycin B.

4.3.7 Nuclear localization function of XRCC4 N326 mutants

Interestingly, we further explored the amino acid asparagine at the position 326 of human XRCC4. XRCC4 at N326 was further analyzed by mutating N326 into various amino acids such as alanine (N326A), glutamine (N326Q) and aspartic acid (N326D). However, none of these mutants showed defective in nuclear localization function like XRCC4 N326L mutant. The lost in nuclear localization function of XRCC4 N326L mutant was similar to that of mutation in nuclear localization signal at XRCC4 K271R mutant (Figure 4-15).

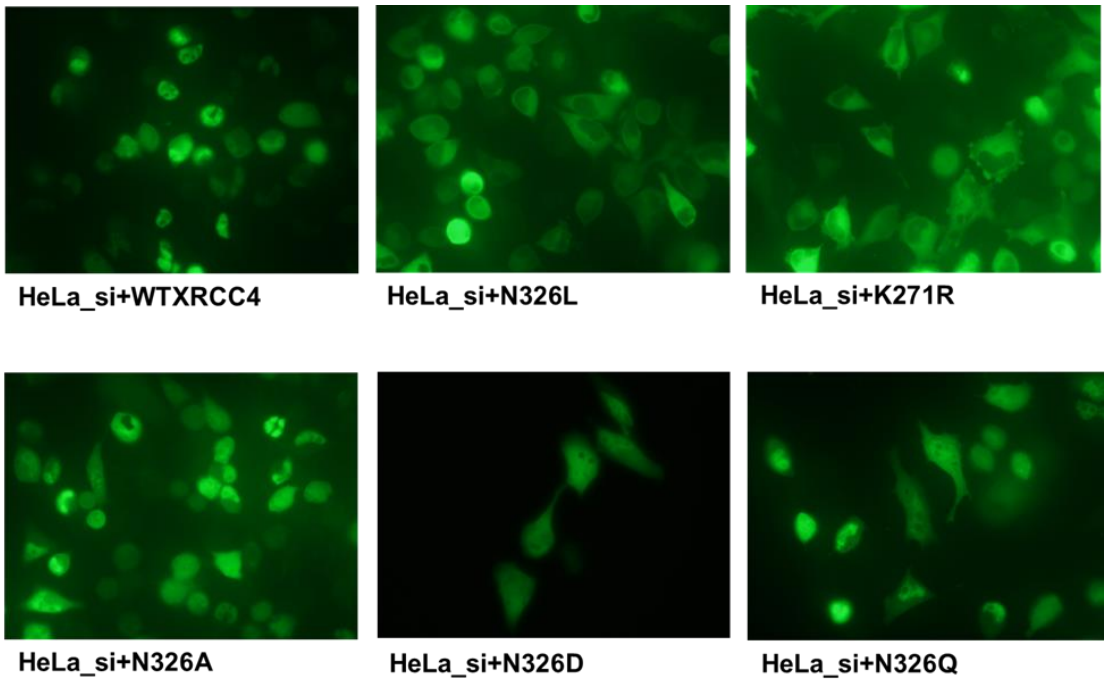

Figure 4 - 10. Subcellular localization of N326 mutants. HeLa cells were first transfected with siRNA directed to 3'-UTR of XRCC4 to knockdown endogenous XRCC4 and then with the expression vectors of wild type XRCC4 or N326 mutants.

4.3.8 Functional deficiency of other XRCC4 N326 mutants

After treatment with γ-irradiation, cell survivability was assessed through colony formation assay. As a result, these three mutants (M10_N326A, M10_N326D and M10_N326Q) showed the radiosensitivity between that of the radioresistant wild-type XRCC4 (M10_WTXRCC4) and the radiosensitive mutated XRCC4 (M10_N326L) (Figure 4-16) (Wanotayan *et al.*, 2015). Further studies, of the significance of XRCC4 at N326 in DNA repair remained to be elucidated.

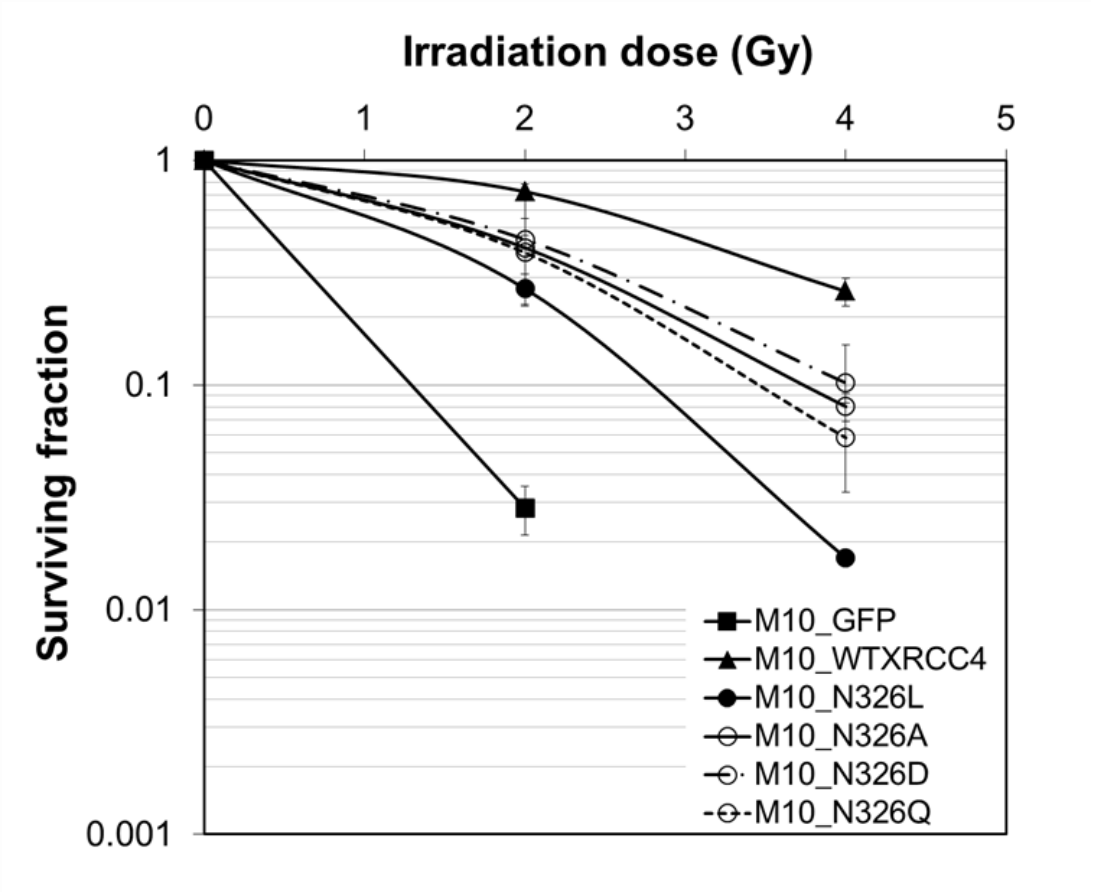

Figure 4 - 11. Survival fraction of N326 mutants (N326A, N326D, N326L and N326Q) after 2 Gy and 4 Gy of γ-irradiation.

4.4 DISCUSSION

Interestingly, in this chapter the results showed that changing Asn326 therein to other amino acids results in reduced XRCC4 function. M10-N326L's sensitivity to ionizing radiation was partly due to its mislocalization in the cytoplasm as found by nuclear localization experiment. Despite XRCC4 protein contains nuclear localization signal, mutation of asparagine 326 (Asn326) into leucine in M10-N326L was found to mimic the leucine-rich nuclear export signal, which was exported outside the nucleus by the nuclear exporter CRM1 resulting in its mislocalization similar to the disruption in nuclear localization signal mutant. However, nuclear localization of M10-N326L mutant was restored by treatment with Leptomycin B, a nuclear export inhibitor, but Leptomycin B could only partially rescue the radiosensitivity of M10-N326L by trapping mutated XRCC4 N326L inside the nucleus promoting the chromatin-bound XRCC4 in binding to the DNA DSB sites of the irradiated cells. Further investigation into Asn326 was performed by changing asparagine to alanine, lysine, aspartic acid or glutamine and established stable mutants. These results collectively indicated that Asn326 would be essential for DSB repair function of XRCC4. It would be noted that Asn326 was conserved among various vertebrate species as analyzed from the retrieval of XRCC4 amino acid sequences suggesting its importance in DSB repair in vertebrates.

CHAPTER 5

EXAMINATION OF THE INTERACTION OF N326L WITH OTHER PROTEINS

(Unpublished part)

CHAPTER 6

CONCLUSION

As XECT domain is highly conserved and is crowded with DNA-PK phosphorylation sites, the significance of XECT domain was elucidated. This study had unexpectedly found an interesting synthetic nuclear export signal by mutating Asn326 into leucine in XRCC4 protein despite the presence of nuclear localization signal. Fractionation study had revealed that XRCC4 N326L mutant with both NLS and synthetic NES was first imported into the nucleus and then exported out by CRM1 as the export was inhibited with the treatment of CRM1 inhibitor, Leptomycin B. Not all the protein with leucine rich region are targeted for the export to the cytoplasm. Next, this study showed that changing Asn326 therein to other amino acids results in reduced XRCC4 function. N326L mutant, which was created initially, was defective in nuclear localization due to synthetic nuclear export signal. However, Leptomycin B, which restored nuclear localization of XRCC4, could only partially rescue the radiosensitivity of M10-N326L.

By mutating Asn326 to either leucine, alanine, aspartic acid or glutamine compromised XRCC4 function in terms of cell survival after irradiation to a certain extent as compared to wild-type XRCC4. It is interesting to note that C-terminal regions of other NHEJ proteins are shown to be essential. Priestley *et al.* showed that deletion of only four amino acids from the C-terminus of DNA-PKcs resulted in great decrease in its function (Priestley *et al,* 1998). Twelve amino acids at the C-terminus of Ku86 are essential for its interaction with DNA-PKcs (Gell and Jackson, 1999; Falck *et al*, 2005). Yano *et al.* elucidated that C-terminus of XLF is shown to be essential for

interaction with Ku. (Yano *et al*, 2011). Considering this, XECT may also act as a module for protein-protein interactions. This present study shed light on the conservation and importance of the XECT region.

REFERENCES

- Alberts B., Bray D., Lewin J., Raff M., Roberts K., Watson J. D., Molecular Biology of the Cell Textbook, Third edition (1994) United States, Garland Publishing Inc.

- Andres, S.N., Modesti, M., Tsai, C.J., Chu, G., Junop, M.S. Crystal structure of human XLF: a twist in nonhomologous DNA end-joining. Molecular Cell 28 (2007) 1093-1101.

- Aziz, K., Nowsheen, S., Pantelias, G., Iliakis, G., Gorgoulis, V.G. Targeting DNA damage and repair: Embracing the pharmacological era for successful cancer therapy. Pharmacology & Therapeutics 133 (2012) 334-350.

- Berg, E., Christensen, M.O., Rosa, I.D., Wannagat, E., Janicke, R.U., Rosner, L.M., Dirks, W.G., Boege, F., Mielke, C. XRCC4 controls nuclear import and distribution of Ligase IV and exchanges faster at damaged DNA in complex with Ligase IV. DNA Repair 10 (2011) 1232-1242.

- Bork, P., Hofmann, K., Bucher, P., Neuwald, A. F., Altschul, S. F., Koonin, E. V. A superfamily of conserved domains in DNA damage-responsive cell cycle checkpoint proteins. FASEB Journal 11 (1997) 68-76.

- Bryans, M., Valenzano., M.C., Stamato, T.D. Absence of DNA ligase IV protein in XR-1 cells+ evidence for stabilization by XRCC4. Mutation Reaseach 433 (1999) 53-58.

- Collis, S.J., DeWeese, T.L., Jeggo, P.A., Parker, A.R. The life and death of DNA-PK: review. Oncogene 24 (2005) 949-961.

- Critchlow, S.E., Bowater R.P., Jackson, S.P. Mammalian DNA double-strand break repair protein XRCC4 interacts with DNA ligase IV. Current Biology 7 (1997) 588-598.

- Dong, X., Biswas, A., Suel, K. E., Jackson, L. K., Martinez, R., Gu, H., Chook, Y. M. Structural basis for leucine-rich nuclear export signal recognition by CRM1. Nature 458 (2009) 1136-1141.

- Falck, J., Coates, J., Jackson, S.P. Conserved modes of recruitment of ATM, ATR and DNA-PKcs to sites of DNA damage. Nature 434 (2005) 605-611.

- Gao, Y., Sun, Y., Frank, K.M., Dikkes, P., Fujiwara, Y., Seidl, K.J., Sekiguchi, J.M., Rathbun, G.A., Swat, W., Wang, J., Bronson, R.T., Malynn, B.A., Bryans, M., Zhu, C., Chaudhuri, J., Davidson, L., Ferrini, R., Stamato, T., Orkin, S.H., Greenberg, M.E., Alt, F.W. A Critical Role for DNA End-Joining Proteins in Both Lymphogenesis and Neurogenesis. Cell 95 (1998) 891-902.

- Gell, D., Jackson, S.P. Mapping of protein-protein interactions within the DNA-dependent protein kinase complex. Nucleic Acids Research 27 (1999) 3494-3502.

- Grawunder, U., Wilm, M., Wu, X., Kulesza, P., Wilson, T.E., Mann, M., Lieber, M.R. Activity of DNA ligase IV stimulated by complex formation with XRCC4 protein in mammalian cells, Nature 388 (1997) 492-495.

- Grawunder, U., Zimmer, D., Kulesza, P., Lieber, M.R. Requirement for an Interaction of XRCC4 with DNA Ligase IV for Wild-type V(D)J Recombination and DNA Double-strand Break Repair in Vivo. The Journal of Biological Chemistry 273 (1998) 24708-24714.

- Hammel, M., Rey, M., Yu, Y., Mani, R.S., Classen, S., Liu, M., Pique, M.E., Fang, S., Mahaney, B.L., Weinfeld, M., Schriemer, D.C., Lees-Miller, S.P., Tainer, J.A. XRCC4 Protein Interactions with XRCC4-like Factor (XLF) Create an Extended Grooved Scaffold for DNA Ligation and Double Strand Break Repair. The Journal of Biological Chemistry 286 (2011) 32638-32650.

- Helleday, T., Lo, J., van Gent, D.C., Engelward, B.P. DNA double-strand break repair: From mechanistic understanding to cancer treatment. DNA Repair 6 (2007) 923-935.

- Ionizing Radiation Fact Book, March 2007, EPA-402-F-06-061, Environmental

Protection Agency, United States.

- Junop, M.S., Modesti, M., Guarne, A., Ghirlando, R., Gellert, M., Yang, W. Crystal structure of the Xrcc4 DNA repair protein and implications for end joining. The EMBO Journal 19 (2000) 5962-5970.

- Kamdar, R.P., Matsumoto, Y. Radiation-induced XRCC4 Association with Chromatin DNA Analyzed by Biochemical Fractionation. Journal of Radiation Research 51 (2010) 303-313.

- Kanno, S., Kuzuoka, H., Sasao, S., Hong, Z., Lan, L., Nakajima, S., Yasui, A. A novel human AP endonuclease with conserved zinc-finger-like motifs involved in DNA strand break responses. The EMBO Journal 26 (2007) 2094-2103.

- Khanna, K.K. and Jackson, S.P. DNA double-strand breaks: signaling, repair and the cancer connection. Nature Genetics 27 (2001) 247-254.

- Kim, J.S., Krasieva, T.B., Kurumizaka, H., Chen, D.J., Taylor, A.M., Yokomori, K. Independent and sequential recruitment of NHEJ and HR factors to DNA damage sites in mammalian cells. The Journal of Cell Biology 170 (2005) 341-347.

- Koch, C.A., Agyei, R., Galicia, S., Metalnikov, P., O'Donnell, P., Starostine, A., Weinfeld, M., Durocher, D. Xrcc4 physically links DNA end processing by

polynucleotide kinase to DNA ligation by DNA ligase IV. The EMBO Journal 23 (2004) 3874-3885.

- Kutay, U. and Guttinger, S. Leucine-rich nuclear-export signals: born to be weak. TRENDS in Cell Biology 15 (2005) 121-124.

- Leber, R., Wise, T.W., Mizuta, R., Meek, K. The XRCC4 Gene Product Is a Target for and Interacts with the DNA-dependent Protein Kinase. The Journal of Biological Chemistry 273 (1998) 1794-1801.

- Lee, K. J., Jovanovic, M., Udayakumar, D., Bladen, C. L., Dynan, W. S. Identification of DNA-PKcs phosphorylation sites in XRCC4 and effects of mutations at these sites on DNA end joining in a cell-free system. DNA Repair 3 (2004) 267-276.

- Lees-Miller, S.P. and Meek K. Repair of DNA double strand breaks by nonhomologous end joining. Biochimie 85 (2003) 1161-1173.

- Li, Z., Otevrel, T., Gao, Y., Cheng, H., Seed, B., Stamato, T.D., Taccioli, G.E., Alt, F.W. The XRCC4 Gene Encodes a Novel Protein Involved in DNA Double-Strand Break Repair and V(D)J Recombination. Cell 83 (1995) 1079-1089.
- Mao, Z., Bozzella, M., Seluanov, A., Gorbunova, V. Comparison of nonhomologous end joining and homologous recombination in human cells. DNA Repair 7 (2008) 1765-1771.

- Matsumoto, Y., Suzuki, N., Namba, N., Umeda, N., Ma, X., Morita, A., Tomita, M., Enomoto, A., Serizawa, S., Hirano, K., Sakai, K., Yasuda, H., Hosoi, Y. Cleavage and phosphorylation of XRCC4 protein induced by X-irradiation. FEBS Letters 478 (2000) 67-71.

- McElhinny, S.A.N., Snowden, C.M., McCarville, J., Ramsden, D.A. Ku Recruits the XRCC4-Ligase IV Complex to DNA Ends. Molecular and Cellular Biology 20 (2000) 2996-3003.

- Mimori, T., Akizuki, M., Yamagata, H., Inada, S., Yoshida, S., Homma, M. Characterization of a high molecular weight acidic nuclear protein recognized by autoantibodies in sera from patients with polymyositis-scleroderma overlap. Journal of Clinical Investigations 68 (1981) 611-620.

- Mizuta, R., Cheng, H., Gao, Y., Alt, F.W. Molecular genetic characterization of XRCC4 function. International Immunology 9 (1997) 1607-1613.

- Modesti, M., Hesse, J.E., Gellert, M. DNA binding of Xrcc4 protein is associated with V(D)J recombination but not with stimulation of DNA ligase IV activity. The EMBO Journal 18 (1999) 2008-2018.
- Modesti, M., Junop, M.S., Ghirlando, R., Rakt, M. van de, Gellert, M., Yang, W., Kanaar, R. Tetramerization and DNA Ligase IV Interaction of the DNA Double-strand Break Repair Protein XRCC4 are Mutually Exclusive. Journal of Molecular

Biology 334 (2003) 215-228.

- Priestley, A., Beamish, H. J., Gell, D., Amatucci, A. G., Muhlmann-Diaz, M. C., Singleton, B. K., Smith, G. C. M., Blunt, T., Schalkwyk, L. C., Bedford, J. S., Jackson, S. P., Jeggo, P. A., Taccioli, G. E. Molecular and biochemical characterisation of DNA-dependent protein kinase-defective rodent mutant irs-20. Nucleic Acids Research 26 (1998) 1965-1973.

- Rich, T., Allen, R.L., Wyllie, A.H. Defying death after DNA damage. Nature 407 (2000) 777-783.

- Sasaki, H., Yoshida, M., Beppu, T. Leptomycin B-induced fixation of X-ray-related potentially lethal damage. Radiation Research 129 (1992) 163-170.

- Sibanda, B.L., Critchlow, S.E., Begun, J., Pei, X.Y., Jackson, S.P., Blundell, T.L., Pellegrini, L. Crystal structure of an Xrcc4-DNA ligase IV complex. Nature Structural Biology 8 (2001) 1015-1019.

- Summers, K.C., Shen, F., Potchanant, S., Phipps, E.A., Hickey, R.J., Malkas, L.H. Phosphorylation: The Molecular Switch of Double-Strand Break Repair. International Journal of Proteomics (2011) doi:10.1155/2011/373816.
- Tyson, J.J. and Novak, B. Regulation of the eukaryotic cell cycle: molecular antagonism, hysteresis, and irreversible transitions. Journal of Theoretical Biology 210 (2001) 249-263.

- Wanotayan, R., Sharma, M.K., Matsumoto, Y. Function of XRCC4 C-terminal Region in DNA Double-Strand Break Repair. Transactions of the American Nuclear Society 111 (2014) 1145-1148.

- Wanotayan, R., Fukuchi, M., Imamichi, S., Sharma, M.K., Matsumoto, Y. Asparagine 326 in the extremely C-terminal region of XRCC4 is essential for the cell survival after irradiation. Biochemical and Biophysical Research Communications 457 (2015) 526-531.

- Ward, J.F. The yield of DNA double-strand breaks produced intracellularly by ionizing radiation: a review. International Journal of Radiation Biology 57 (1990) 1141-1150.

- Yano, K., Morotomi-Yano, K., Lee, K.J., Chen, D.J. Functional significance of the interaction with Ku in DNA double-strand recognition of XLF. FEBS Letters 585 (2011), 841-846.

- Yu, Y., Wang, W., Ding, Q., Ye, R., Chen, D., Merkle, D., Schriemer, D., Meek, K., Lees-Miller S.P. DNA-PK phosphorylation sites in XRCC4 are not required for survival after radiation or for V(D)J recombination. DNA Repair 3 (2003) 1239-

1252.

APPENDIX

XRCC4 PROTEIN IN MAMMALS

Species	Scientific name	Protein ID	Identities	Organism
Human	Homo sapiens	BAB20668.1		Eukaryota; Metazoa; Chordata; Craniata; Vertebrata; Euteleostomi; Mammalia; Eutheria; Euarchontoglires; Primates; Haplorrhini; Catarrhini; Hominidae; Homo.
		BAF83428.1	336/336(100%)	
		AAC50339.1	333/336(99%)	
Western gorilla	Gorilla gorilla	ADQ01151.1	329/336(98%)	Eukaryota; Metazoa; Chordata; Craniata; Vertebrata; Euteleostomi; Mammalia; Eutheria; Euarchontoglires; Primates; Haplorrhini; Catarrhini; Hominidae; Gorilla.
		XP_004042287.1	293/297(99%)	
Chimpanzee	Pan troglodytes	BAK63102.1	328/336(98%)	Eukaryota; Metazoa; Chordata; Craniata; Vertebrata; Euteleostomi; Mammalia; Eutheria; Euarchontoglires; Primates; Haplorrhini; Catarrhini; Hominidae; Pan.
		XP_001148037.1	330/336(98%)	
pygmy chimpanzee	Pan paniscus	XP_003822293.1	331/336(99%)	Eukaryota; Metazoa; Chordata; Craniata; Vertebrata; Euteleostomi; Mammalia; Eutheria; Euarchontoglires; Primates; Haplorrhini; Catarrhini; Hominidae; Pan.
crab-eating macaque	Macaca fascicularis	BAE01181.1	315/336(94%)	Eukaryota; Metazoa; Chordata; Craniata; Vertebrata; Euteleostomi; Mammalia; Eutheria; Euarchontoglires; Primates; Haplorrhini; Catarrhini; Cercopithecidae; Cercopithecinae; Macaca.
Rhesus monkey	Macaca mulatta	XP_001111862.1	315/336(94%)	Eukaryota; Metazoa; Chordata; Craniata; Vertebrata; Euteleostomi; Mammalia; Eutheria; Euarchontoglires; Primates; Haplorrhini; Catarrhini; Cercopithecidae; Cercopithecinae; Macaca.
		XP_001111757.1	318/336(95%)	
Bolivian squirrel monkey	Saimiri boliviensis boliviensis	XP_003920835.1	306/336(91%)	Eukaryota; Metazoa; Chordata; Craniata; Vertebrata; Euteleostomi; Mammalia; Eutheria; Euarchontoglires; Primates; Haplorrhini; Platyrrhini; Cebidae; Saimiriinae; Saimiri.
Sumatran orangutan	Pongo abelii	ADQ01144.1	326/336(97%)	Eukaryota; Metazoa; Chordata; Craniata; Vertebrata; Euteleostomi; Mammalia; Eutheria; Euarchontoglires; Primates; Haplorrhini; Catarrhini; Hominidae; Pongo.
		CAH91936.1	45/47(96%)	
		NP_001126122.2	326/336(97%)	
Horse	Equus caballus	XP_001504688.1	269/336(80%)	Eukaryota; Metazoa; Chordata; Craniata; Vertebrata; Euteleostomi; Mammalia; Eutheria; Laurasiatheria; Perissodactyla; Equidae; Equus.

XRCC4 PROTEIN IN MAMMALS

Species	Scientific name	Protein ID	Identities	Organism
Dog	Canis familiaris	XP_849518.1	266/336(79%)	Eukaryota; Metazoa; Chordata; Craniata; Vertebrata; Euteleostomi; Mammalia; Eutheria; Laurasiatheria; Carnivora; Caniformia; Canidae; Canis.
House mouse	Mus musculus	BAB62316.1 XP_001471793.1	248/334(74%) 249/334(75%)	Eukaryota; Metazoa; Chordata; Craniata; Vertebrata; Euteleostomi; Mammalia; Eutheria; Euarchontoglires; Glires; Rodentia; Sciurognathi; Muroidea; Muridae; Murinae; Mus; Mus.
Pig	Sus scrofa	XP_003123809.1	241/301(80%)	Eukaryota; Metazoa; Chordata; Craniata; Vertebrata; Euteleostomi; Mammalia; Eutheria; Laurasiatheria; Cetartiodactyla; Suina; Suidae; Sus.
Norway rat	Rattus norvegicus	NP_001007000.1	235/334(70%)	Eukaryota; Metazoa; Chordata; Craniata; Vertebrata; Euteleostomi; Mammalia; Eutheria; Euarchontoglires; Glires; Rodentia; Sciurognathi; Muroidea; Muridae; Murinae; Rattus.
gray short-tailed opossum	Monodelphis domestica	XP_001369113.2 XP_001369113.1	209/336(62%) 183/297(62%)	Eukaryota; Metazoa; Chordata; Craniata; Vertebrata; Euteleostomi; Mammalia; Metatheria; Didelphimorphia; Didelphidae; Monodelphis.
platypus	Ornithorhynchus anatinus	XP_001511773.2 XP_001511773.1	169/294(57%) 153/257(60%)	Eukaryota; Metazoa; Chordata; Craniata; Vertebrata; Euteleostomi; Mammalia; Monotremata; Ornithorhynchidae; Ornithorhynchus.
Cattle	Bos taurus	NP_001075084.1	263/336(78%)	Eukaryota; Metazoa; Chordata; Craniata; Vertebrata; Euteleostomi; Mammalia; Eutheria; Laurasiatheria; Cetartiodactyla; Ruminantia; Pecora; Bovidae; Bovinae; Bos.
white-tufted-ear marmoset	Callithrix jacchus	NP_001254694.1	297/336(88%)	Eukaryota; Metazoa; Chordata; Craniata; Vertebrata; Euteleostomi; Mammalia; Eutheria; Euarchontoglires; Primates; Haplorrhini; Platyrrhini; Cebidae; Callitrichinae; Callithrix.
northern white-cheeked gibbon	Nomascus leucogenys	XP_003261603.1	327/336(97%)	Eukaryota; Metazoa; Chordata; Craniata; Vertebrata; Euteleostomi; Mammalia; Eutheria; Euarchontoglires; Primates; Haplorrhini; Catarrhini; Hylobatidae; Nomascus.

XRCC4 PROTEIN IN MAMMALS

Species	Scientific name	Protein ID	Identities	Organism
olive baboon	Papio anubis	XP_003899945.1	320/336(95%)	Eukaryota; Metazoa; Chordata; Craniata; Vertebrata; Euteleostomi; Mammalia; Eutheria; Euarchontoglires; Primates; Haplorrhini; Catarrhini; Cercopithecidae; Cercopithecinae; Papio.
domestic guinea pig	Cavia porcellus	XP_003479527.1	248/336(74%)	Eukaryota; Metazoa; Chordata; Craniata; Vertebrata; Euteleostomi; Mammalia; Eutheria; Euarchontoglires; Glires; Rodentia; Hystricognathi; Caviidae; Cavia.
southern white rhinoceros	Ceratotherium simum simum	XP_004420452.1	268/336(80%)	Eukaryota; Metazoa; Chordata; Craniata; Vertebrata; Euteleostomi; Mammalia; Eutheria; Laurasiatheria; Perissodactyla; Rhinocerotidae; Ceratotherium.
star-nosed mole	Condylura cristata	XP_004678486.1	218/336(65%)	Eukaryota; Metazoa; Chordata; Craniata; Vertebrata; Euteleostomi; Mammalia; Eutheria; Laurasiatheria; Insectivora; Talpidae; Condylura.
nine-banded armadillo	Dasypus novemcinctus	XP_004483495.1	234/297(79%)	Eukaryota; Metazoa; Chordata; Craniata; Vertebrata; Euteleostomi; Mammalia; Eutheria; Xenarthra; Cingulata; Dasypodidae; Dasypus.
small Madagascar hedgehog	Echinops telfairi	XP_004703707.1	212/352(60%)	Eukaryota; Metazoa; Chordata; Craniata; Vertebrata; Euteleostomi; Mammalia; Eutheria; Afrotheria; Tenrecidae; Tenrecinae; Echinops.
naked mole-rat	Heterocephalus glaber	XP_004841699.1	249/336(74%)	Eukaryota; Metazoa; Chordata; Craniata; Vertebrata; Euteleostomi; Mammalia; Eutheria; Euarchontoglires; Glires; Rodentia; Hystricognathi; Bathyergidae; Heterocephalus.
lesser Egyptian jerboa	Jaculus jaculus	XP_004651494.1	238/336(71%)	Eukaryota; Metazoa; Chordata; Craniata; Vertebrata; Euteleostomi; Mammalia; Eutheria; Euarchontoglires; Glires; Rodentia; Sciurognathi; Dipodidae; Dipodinae; Jaculus.
domestic ferret	Mustela putorius furo	XP_004799716.1	263/336(78%)	Eukaryota; Metazoa; Chordata; Craniata; Vertebrata; Euteleostomi; Mammalia; Eutheria; Laurasiatheria; Carnivora; Caniformia; Mustelidae; Mustelinae; Mustela.

XRCC4 PROTEIN IN MAMMALS

Species	Scientific name	Protein ID	Identities	Organism
American pika	Ochotona princeps	XP_004586357.1	224/297(75%)	Eukaryota; Metazoa; Chordata; Craniata; Vertebrata; Euteleostomi; Mammalia; Eutheria; Euarchontoglires; Glires; Lagomorpha; Ochotonidae; Ochotona.
killer whale	Orcinus orca	XP_004281685.1	275/336(82%)	Eukaryota; Metazoa; Chordata; Craniata; Vertebrata; Euteleostomi; Mammalia; Eutheria; Laurasiatheria; Cetartiodactyla; Cetacea; Odontoceti; Delphinidae; Orcinus.
small-eared galago	Otolemur garnettii	XP_003786006.1	271/336(81%)	Eukaryota; Metazoa; Chordata; Craniata; Vertebrata; Euteleostomi; Mammalia; Eutheria; Euarchontoglires; Primates; Strepsirrhini; Lorisiformes; Galagidae; Otolemur.
Pacific walrus	Odobenus rosmarus divergens	XP_004405679.1	271/336(81%)	Eukaryota; Metazoa; Chordata; Craniata; Vertebrata; Euteleostomi; Mammalia; Eutheria; Laurasiatheria; Carnivora; Caniformia; Odobenidae; Odobenus.
sheep	Ovis aries	XP_004009114.1	267/336(79%)	Eukaryota; Metazoa; Chordata; Craniata; Vertebrata; Euteleostomi; Mammalia; Eutheria; Laurasiatheria; Cetartiodactyla; Ruminantia; Pecora; Bovidae; Caprinae; Ovis.
Tasmanian devil	Sarcophilus harrisii	XP_003759919.1	218/336(65%)	Eukaryota; Metazoa; Chordata; Craniata; Vertebrata; Euteleostomi; Mammalia; Metatheria; Dasyuromorphia; Dasyuridae; Sarcophilus.
European shrew	Sorex araneus	XP_004613226.1	247/336(74%)	Eukaryota; Metazoa; Chordata; Craniata; Vertebrata; Euteleostomi; Mammalia; Eutheria; Laurasiatheria; Insectivora; Soricidae; Soricinae; Sorex.
Florida manatee	Trichechus manatus latirostris	XP_004388894.1	266/336(79%)	Eukaryota; Metazoa; Chordata; Craniata; Vertebrata; Euteleostomi; Mammalia; Eutheria; Afrotheria; Sirenia; Trichechidae; Trichechus.

XRCC4 PROTEIN IN OTHER SPECIES

Species	Scientific name	Protein ID	Identities	Organism
western clawed frog	Xenopus tropicalis	NP_001106551.1	161/346(47%)	Eukaryota; Metazoa; Chordata; Craniata; Vertebrata; Euteleostomi; Amphibia; Batrachia; Anura; Pipoidea; Pipidae; Xenopodinae; Xenopus; Silurana.
African clawed frog	Xenopus laevis	NP_001085360.1	166/373(45%)	Eukaryota; Metazoa; Chordata; Craniata; Vertebrata; Euteleostomi; Amphibia; Batrachia; Anura; Pipoidea; Pipidae; Xenopodinae; Xenopus; Xenopus.
chicken	Gallus gallus	XP_424905.4	183/341(54%)	Eukaryota; Metazoa; Chordata; Craniata; Vertebrata; Euteleostomi; Testudines + Archosauria group; Archosauria; Dinosauria; Saurischia; Theropoda; Coelurosauria; Aves; Neognathae; Galliformes; Phasianidae; Phasianinae; Gallus.
zebrafish	Danio rerio	NP_957080.1	130/357(36%)	Eukaryota; Metazoa; Chordata; Craniata; Vertebrata; Euteleostomi; Actinopterygii; Neopterygii; Teleostei; Ostariophysi; Cypriniformes; Cyprinidae; Danio.
thale cress	Arabidopsis thaliana	NP_001154639.1	49/189(26%)	Eukaryota; Viridiplantae; Streptophyta; Embryophyta; Tracheophyta; Spermatophyta; Magnoliophyta; eudicotyledons; core eudicotyledons; rosids; malvids; Brassicales; Brassicaceae; Camelineae; Arabidopsis.
mallard	Anas platyrhynchos	XP_005012948.1	181/341(53%)	Eukaryota; Metazoa; Chordata; Craniata; Vertebrata; Euteleostomi; Testudines + Archosauria group; Archosauria; Dinosauria; Saurischia; Theropoda; Coelurosauria; Aves; Neognathae; Anseriformes; Anatidae; Anas.
bread wheat	Triticum aestivum	AEJ83861.1	54/227(24%)	Eukaryota; Viridiplantae; Streptophyta; Embryophyta; Tracheophyta; Spermatophyta; Magnoliophyta; Liliopsida; Poales; Poaceae; BEPclade; Pooideae; Triticeae; Triticum.
zebra finch	Taeniopygia guttata	XP_002190026.2	125/214(58%)	Eukaryota; Metazoa; Chordata; Craniata; Vertebrata; Euteleostomi; Testudines + Archosauria group; Archosauria; Dinosauria; Saurischia; Theropoda; Coelurosauria; Aves; Neognathae; Passeriformes; Passeroidea; Estrildidae; Estrildinae; Taeniopygia.